REPORT DOCUMENTATION PAGE

Form Approved OMB NO. 0704-0188

1. REPORT DATE (DD-MM-YYYY)	2. REPORT TYPE	3. DATES COVERED (From - To)
23-04-2009	Final Report	9-Jul-2004 - 8-Jan-2008

4. TITLE AND SUBTITLE

New Fluorinated and Sulfonated Block Copolymers: Final Report

5a. CONTRACT NUMBER
W911NF-04-1-0329

5b. GRANT NUMBER

5c. PROGRAM ELEMENT NUMBER
611102

6. AUTHORS

Samuel P. Gido, Jimmy W. Mays

5d. PROJECT NUMBER

5e. TASK NUMBER

5f. WORK UNIT NUMBER

7. PERFORMING ORGANIZATION NAMES AND ADDRESSES

University of Massachusetts - Amherst
Office of Grant & Contract Admin.
408 Goodell Building
Amherst, MA   01003 -3285

8. PERFORMING ORGANIZATION REPORT NUMBER

9. SPONSORING/MONITORING AGENCY NAME(S) AND ADDRESS(ES)

U.S. Army Research Office
P.O. Box 12211
Research Triangle Park, NC 27709-2211

10. SPONSOR/MONITOR'S ACRONYM(S)
ARO

11. SPONSOR/MONITOR'S REPORT NUMBER(S)
46608-CH.1

12. DISTRIBUTION AVAILIBILITY STATEMENT

Approved for public release; Distribution Unlimited

13. SUPPLEMENTARY NOTES

The views, opinions and/or findings contained in this report are those of the author(s) and should not contrued as an official Department of the Army position, policy or decision, unless so designated by other documentation.

14. ABSTRACT

A new class of fluorinated and sulfonated block copolymers was synthesized and characterized with respect to morphology using TEM and small angle X-ray and neutron scattering. Proton and methanol transport properties were evaluated with a view toward using these materials for fuel cell membranes. The materials formed microphase separated morphologies, which were generally less well ordered than unfluorinated and sulfonated block copolymers. It was possible, however, to get some morphological alignment in the materials by application of an

15. SUBJECT TERMS

Block Copolymer, Polyelectrolyte, fuel cell, morphology, polymer synthesis

16. SECURITY CLASSIFICATION OF:			17. LIMITATION OF ABSTRACT	15. NUMBER OF PAGES	19a. NAME OF RESPONSIBLE PERSON
a. REPORT	b. ABSTRACT	c. THIS PAGE	SAR		Samuel Gido
U	U	U			19b. TELEPHONE NUMBER
					413-577-1216

5   **Materials Comprising Polydienes and Hydrophilic Polymers and Related Methods**

Patent Filed in US? (5d-1)   Y

Patent Filed in Foreign Countries? (5d-2)   N

Was the assignment forwarded to the contracting officer? (5e)   N

Foreign Countries of application (5g-2):

    5a: Jimmy W. Mays

  5f-1a: University of Tennessee

   5f-c:

    5a: Suxiang Deng

  5f-1a: University of Tennessee

   5f-c:

    5a: Samuel P. Gido

  5f-1a: University of Massachusettts Amherst

   5f-c:

    5a: Mohammed K. Hassan

  5f-1a: University of Southern Mississippi

   5f-c:

    5a: Kenneth A. Mauritz

  5f-1a: University of Southern Mississippi

   5f-c:

New Fluorinated and Sulfonated Block Copolymers Final Report

Samuel P. Gido
Jimmy W. Mays

Papers Published In Peer Reviewed Journals

1.   Yuqing Zhu, Engin Burgaz, Samuel P. Gido*, Ulrike Staudinger and Roland Weidisch*, David Uhrig, and Jimmy W. Mays "Morphology and Tensile Properties of Multigraft Copolymers With Regularly Spaced Tri-, Tetra- and Hexa-functional Junction Points" *Macromolecules* **2006**, *39*, 4428-4436.

2.   Abuzaina FM, Garetz BA, Patel AJ, Newstein MC, Gido SP, Hu XC, Balsara NP "Observation of nematic texture in a diblock copolymer melt" *Macromolecules* **2006**, *39*, 3377-3385.

3.   Staudinger U, Weidisch R, Zhu Y, Gido SP, Uhrig D, Mays JW, Iatrou H, Hadjichristidis N. "Mechanical properties and hysteresis behaviour of multigraft copolymers" *Macromolecular Symposia* **2006**, *233*, 42-50.

4.   Mamodia M (Mamodia, Mohit), Panday A (Panday, Ashoutosh), Gido SP (Gido, Samuel P.), Lesser AJ (Lesser, Alan J.) "Effect of microdomain structure and process conditions on the mechanical Behavior of cylindrical block copolymer systems" *Macromolecules* 40 (20): 7320-7328, **2007**

5.   Wang XY (Wang, Xiaoyu)1, Sandman DJ (Sandman, Daniel J.), Chen SJ (Chen, Shujun), Gido SP (Gido, Samuel P.) "Thermochromic polydiacetylene micro- and nanocrystals: An unusual size effect in electronic spectra" *Macromolecules* 41, 773-778, **2008**

6.   Samuel P. Gido*, and Ashoutosh Panday. "Azimuthal Orientational Correlations due to Excluded Volume Epitaxy in Growing Anisotropic Grains" *Philosophical Magazine* 2009, 89(9), 771-787.

Presentations at Meetings

1.   Ashoutosh Panday, Samuel Gido. "Shape Templating Effects Among Growing Anisotropic Particles." American Physical Society National Meeting. Los Angeles, CA. March 24, 2005.

2.   Ashoutosh Panday, Samuel Gido, Kunlun Hong, Jimmy Mays. "Stability of Core-Shell-Cylinder Structure of Poly(styrene-b-1,3-cyclohexadiene) Diblock Copolymers." American Physical Society National Meeting. Los Angeles, CA. March 21, 2005.

3.   Shujun Chen, Samuel P. Gido. "Morphological Transitions in a Triblock Copolymer and Its Sulfonated Ionomer: Thermal Annealing and Solvent Effects." American Physical Society National Meeting. Los Angeles, CA. March 21, 2005.

4.   Akinbode Isaacs-Sodeye, Shujun Chen, Samuel Gido. "Electric Field induced alignment and morphological transitions of triblock copolymers." American Physical Society National Meeting. Los Angeles, CA. March 21, 2005.

5.   Xiaochuan Hu, Samuel Gido, Thomas Russell, Hermis Iatrou, Nikos Hadjichristidis, Ferass Abuzaina, Bruce Garetz. "Grain Growth Kinetics of AnBn Star Block Copolymers in Supercritical Carbon Dioxide." American Physical Society National Meeting. Los Angeles, CA. March 23, 2005.

6.   "Synthesis, Morphology, and Tensile Properties of Multigraft Copolymers with Regularly Spaced Tri-, Tetra-, and Hexa-functional Junction Points", D. Uhrig, J. W. Mays, Y. Zhu, E. Burgaz, S. P. Gido, U. Staudinger, and R. Weidisch, poster presentation at the 19th International Symposium on Polymer Analysis and Characterization (ISPAC), Oak Ridge, Tennessee, June 12 - 14, 2006.

7.   "Synthesis and Morphology of Fluorinated and Sulfonated Block Copolymers", J. W. Mays, T. Huang, and S. P. Gido, presented at the National Meeting of the American Chemical Society, Atlanta, GA, March 26 - 30, 2006; see also: Polym. Mater. Sci. Eng., 94, 165-166 (2006).

8.   American Physical Society National Meeting, Baltimore, Maryland March 2006: Session K25: Polymer Electrolytes and Conduction, Tuesday, March 14, 2006, "Proton Conducting Membranes from Fluorinated Poly(Isoprene)-{block}-Sulphonated Poly(Styrene): A Structure Vs Property Study" Akinbode Isaacs-Sodeye, Samuel Gido, Tianzi Huang,Jimmy Mays

9.   American Physical Society National Meeting, Baltimore, Maryland March 2006: Session V30: Focus Session: Mechanical Properties: Microscale Deformation and Failure, March 16, 2006 "Tensile Properties and Hysteresis Behavior of Graft Copolymers with Complex Molecular Architecture" R. Weidisch, U. Staudinger, Y. Zhu, S.P. Gido, D. Uhrig, J.W. Mays, N. Hadjichristidis,H. Iatrou

10.   American Physical Society National Meeting, Baltimore, Maryland March 2006: Session H24: Polymers at Interfaces, March 14, 2006 "Defects in a Noncentrosymmetric Lamellar Block Copolymer Blends" Shujun Chen, Samuel P. Gido, Thodoris Tsoukatos, Apostolos Avgeropoulos, Nikos Hadjichristidis, Kunlun Hong, Jimmy W. Mays.

11.   American Physical Society National Meeting, Baltimore, Maryland March 2006: Session N30: Block Copolymer Phase Behavior, March 15, 2006, "Azimuthal Orientational Correlations due to Excluded Volume Epitaxy in Growing Anisotropic Grains" Ashoutosh Panday, Samuel Gido.

12.   American Physical Society National Meeting, Baltimore, Maryland March 2006: Session C1: Poster Session I, March 13, 2006 "Morphology of Fluorinated and Sulfonated diblock Copolymers" Tomonori Hosoda, Sam Gido, Tianzi Huang, Jimmy Mays.

13.   American Physical Society National Meeting, Baltimore, Maryland March 2006: Session C1: Poster Session I, March 13, 2006 "Scaling of Avrami Kinetics of Growing Anisotropic Grains" Samuel Gido, Ashoutosh Panday.

14.   American Physical Society National Meeting, Denver, Colorado March 2007: Session A17: Charged and Ion Containing Polymers, March 5, 2007. "Proton Conducting Membranes from Fluroinated Poly(Isoprene-b-sulfonated polystyrene): Structure and Transport Properties. Akinbode Isaacs-Sodeye, Samuel Gido.

15.   American Physical Society National Meeting, Denver, Colorado March 2007: Session L24: John H. Dillion Award Symposium, March 6, 2007. "Branched Block Copolymers: Morphology, Properties, and Applications" Samuel P. Gido

21. American Physical Society National Meeting, Denver, Colorado March 2007: Session W24: Microphysical Properties of Block Copolymer Aggregates, Going Beyond Structure, March 8, 2007. "Superelastric materials based on multigraft copolymers" U. Staudinger, R. Weidisch, Y. Zhu, S. P. Gido, D. Uhrig, J. W. Mays, M. Klueppel, G. Heinrich.

(5.1) POLYMER ELECTROLYTE MEMBRANES FROM FLUORINATED POLY(ISOPRENE*)*-BLOCK-SULFONATED POLY(STYRENE): MEMBRANE STRUCTURE AND TRANSPORT PROPERTIES

Abstract

With a view to optimizing morphology and ultimately properties, membranes have been cast from relatively inexpensive block-copolymer ionomers of fluorinated poly(Isoprene*)-block-*sulfonated poly(Styrene) (FISS) with various sulfonation levels, in both the acid form and the cesium neutralized form. The morphology of these membranes were characterized by TEM and USAXS, as well as water uptake, proton conductivity and methanol permeability within the temperature range from 20 to 60°C. Random phase separated morphologies were obtained for all samples exept the cesium sample with 50mol% sulfonation. The transport properties increased with increasing degree of sulfonation and temperature for all samples. The acid form samples absorbed more water than the cesium samples with a maximum swelling of 595% recorded at 60°C for the acid sample with 50mol% sulfonation. Methanol permeability for the latter sample was more than an order of magnitude less than for Nafion 112 but so was the proton conductivity at 20°C within the plane of the membrane. Across the plane of the membrane this sample had half the conductivity of Nafion 112 at 60°C.

Introduction

Alternative sources of energy, besides fossil fuels, are a pressing need in the world we live in today. One such promising alternative is a fuel cell. Fuel Cells are typically classified according to their type of membrane, which serve both as a cell separator and a proton conductor[1]. Two of the existing types of fuel cell membranes use polymers namely, Polymer Electrolyte Membrane Fuel Cells (PEMFC) and Direct Methanol Fuel Cells (DMFC)

The DMFC can be seen as a variant of the PEMFC. The membranes are typically the same; however, the feed for DMFC is methanol in an aqueous 1-2 M solution or in its vapor form. This fuel cell type has the most promise for portable applications as system complexities are reduced since there is no need to reform or store hydrogen, and the existing liquid fuels infrastructure can be used for methanol. Catalysts, as well as operating temperature ranges, are very similar to the PEMFC. Widespread commercialization of such devices has been impeded by factors including catalyst cost, mechanical or chemical instability and poor selectivity of the Polymer Electrolyte Membranes (PEM)[2]. Selectivity issues arise from the cross-over of methanol from the anode to the cathode, which closely tracks water based proton conductivity, ultimately reducing cell efficiencies.

Nafion[TM], which is the prototypical PEM material, has a hydrophobic fluoropolymer backbone and hydrophilic fluorosulfonic acid bearing side chains[3,4]. At present it is costly and still exhibits poor selectivity in DMFC applications. This has led to a concerted effort to develop alternatives[5-11]. These materials range from fluoropolymer to aromatic to hydrocarbon backboned materials, bearing pendant acid groups in one configuration or another.

Block copolymer ionomers are one such category gaining interest. As in normal block copolymers, nanometer scale microphase separation occurs, creating separate hydrophobic and ion-cluster containing hydrophilic domains with similar morphological diversity to neutral block copolymers. These phase separated systems have been shown to yield greater conductivity than the more homogeneous structures from random copolymers [5]. Also having random phase separated domains in these systems has been shown to give better transport properties than in systems where well ordered domains do not line up with direction of transport[12,13]. Furthermore block copolymer ionomers with one block being a fluoropolymer have been shown to exhibit enhanced network formation and mechanical integrity especially when hydrated[5].

Swelling or dilation of ionomers upon increasing water or methanol content and at service temperatures is also an important factor affecting conductivity and mechanical integrity. Backbone stiffness and counterions attached to the acid sites are known to affect the degree of water uptake and, hence swelling[3]. Upon neutralizing Nafion[TM] from its acid form to its Cesium form, one study has shown decreased water uptake and methanol permeability, due to its lower hydration energy and hence water uptake[14].

With a view to developing inexpensive phase separated PEMs we have synthesized, block copolymer ionomers comprising of a fluorinated hydrophobic block

and a partially sulfonated hydrophilic block by means of post polymerization modification of the common poly(Styrene)-*block*-poly(Isoprene). The structures of membranes fabricated from these material as well as their transport properties (i.e proton conductivity and methanol permeability) have been investigated under conditions mimicking fuel cell usage, to assess their viability for low temperature DMFC applications. Also being synthesized from anionically polymerized precursors these materials will serve as suitable model molecules with precise architectures, to study the relationships between chemical structure and morphology.

Experimental Section

Materials

The synthetic procedure and characterization for fluorinated poly(Isoprene)-block- sulfonated poly(Styrene) (FISS) materials have been described in detail elsewhere[15]. The precursor poly(Styrene)-block- poly(Isoprene) (PS-PI) diblock copolymer used in this work was anionically polymerized, having reported properties: Mw =31,000 ,PDI=1.05, 27mol% PS. Fluorinated samples were sulfonated to 23,28 and 50 mol%, as determined by ^{1}H NMR. Some samples were neutralized to the cesium salt form , and the balance left in the acid form. The cesium form facilitates contrast in the x-ray scattering experiments, besides exhibiting different transport properties. A sample coded FISS-AC50 would refer to the acid form of the material, sulfonated to 50mol% of the styrene units in the PS block. Nafion^{TM} 112 was generously donated by Atofina Chemicals Inc., and was pretreated to the acid form according to the procedure reported elsewhere[16].

Preparation of Membranes

Freeze dried FISS samples were dissolved in a mixture of Toluene/N-methylformamide(TOL/NMF:85/15 (w/w)) with a concentration ranging from 12-15 wt%. The NMF was used as a polar cosolvent. These solutions were then cast unto glass plates for a day in the fume hood at room temperature for rapid casting of kinetically trapped disordered morphology. Subsequently they were placed in an oven for 1 day at 60°C, and finally in the oven at 60°C plus vacuum for a day to remove most residual solvent. The acid form samples were further reactivated by soaking overnight in a 2M aqueous HCL solution containing methanol (20v/v) to enhance swelling and acid permeation. They were thereafter rinsed repeatedly in deionized water until PH was neutralized and then dried at 60°C in a vacuum oven for a day, and again in vacuum plus 60°C for one day. Cast membranes were subsequently removed and stored in airtight bags for further usage. Dry membrane thicknesses were measured using a digital micrometer and range from 60-90 um. The Nafion 112 samples were also rinsed until PH was neutralized and then dried at 60°C in a vacuum oven for a day and stored in the same way.

Structural Characterization

The morphology of the dry membranes were determined by transmission electron microscopy (TEM). The membranes were first coated with gold and carbon on both sides, to serve as marker and epoxy diffusion barrier respectively. They were subsequently embedded in epoxy(Araldite 516) and 50 nm thin sections of samples were

cut across the thickness of the membrane using a Leica Ultracut UCT cryomicrotome at -120°C. These were then collected on copper grids and stained with RuO_4 vapor for 1 hour. It is assumed that only the unsulfonated Polystyrene domains were stained. TEM images were obtained using a JEOL-2010 microscope operating at an accelerating voltage of 200Kv. In the bright field mode.

Small angle x-ray scattering(SAXS) was performed at the Advanced Photon Source(APS) in Argonne National Laboratory on beamline 32-ID, fitted with a Bonse-Hart camera typically used for ultra small angle x-ray scattering (USAXS), which has been described elsewhere[17]. The x-ray energies range from 7 to 18 keV, yielding a q range from 0.0001 to 1.0 A^{-1} (where q, the scattering vector is equal to $4\pi\sin(\theta)/\lambda$, where 2θ is the scattering angle and λ is the wavelength of the incident radiation). The beam size was 1mm x 2mm, and a 1-dimensional photodiode detector was used. Air-blanks were subtracted and slit desmearing of the resulting data was carried out using the lake method. All SAXS data were collected with the samples in the transmission position, with membrane normal in the direction of the beam.

In order to determine the surface morphology of the membranes, which significantly affects the interfacial properties in both Proton and methanol transport measurements, scanning probe microscopy (SPM) technique was used. SPM images of both sides of each membrane were collected using a Digital Instruments Dimension^{TM} 3100 Atomic Force Microscope (a type of SPM) in the tapping mode.

Transport Properties
The water uptake behavior of the membranes were determined by soaking the samples in deionized water for at least 16 hours each at both room temperature(20°C) and 60°C. The difference in weight from dry to wet state was measured using a weighing scale accurate to 0.01 mg. The amount of water uptake was then calculated according to the expression:

$$WaterUptake(\%) = \frac{W_{Wet} - W_{Dry}}{W_{Dry}} \times 100 \tag{1}$$

Where W_{Wet} and W_{Dry} are the weights of wet and dry samples respectively. The permeation of methanol was measured using a horizontal diffusion cell, procured from Permegear Inc. the whole experimental setup is shown in the Schematic in Figure 1 below.

The cell was customized to have two 5ml ,jacketed chambers side by side, between which a membrane was clamped after being soaked in deionized water for at least a week. Holes in between the chambers allowed for 0.502 cm^2 of active membrane area exposed to 2M aqueous methanol solution on the feed side and HPLC grade water on the receiving side. Two ports in the receiving side allowed for continuous recirculation of content at a rate of 100ul/min, through a Waters 410 differential refractometer with voltage signal output to a National Instruments data acquisition interface sampling at a

rate of 20,000 Hz. The voltage signal was calibrated to reflect changes in methanol concentration on the receiving side. Contents of both chambers were stirred continuously and water from a bath recirculation through the thermal jackets surrounding the chambers was used to control the temperature. The procedure was according to the technique reported by Elabd et al. with the difference being the detection method[18].

Upon solving the equation for one-dimensional diffusion through a plane sheet and rearranging, the expression below can be used to determine the permeability of methanol through membranes of different thicknesses at early times.

$$\frac{C_B(t)V_B L}{C_A A} = P\left(t - \frac{L^2}{6D}\right) \tag{2}$$

Where C_A and C_B are the methanol concentrations in the feed and receiving chambers and the condition $C_A \gg C_B$ is satisfied. A and L represent the membrane area exposed to fluid and its thickness, while V_B is the volume of the receiving chamber. P represents the permeability of methanol through the membrane and is calculated as the slope of $[(C_B(t) V_B L)/ (C_A A)]$ versus time. P is equivalent to the product of the membrane diffusion and partition coefficients, D and K respectively [18,19].

.

Proton (and cesium) conductivity of the membranes were measured by means of four and two probe complex impedance spectroscopy techniques, which measure conductivity within and normal to the plane of the membrane respectively. A solartron 1252A frequency response analyzer linked to a an SI 1287 electrochemical interface was used within a frequency range of 0.1 and 300KHz.The 4 probe used was similar to that described in literature[20], however graphite paper strips were used as the blocking electrode. The 0.5 x 3cm membrane samples were initially soaked in deionized water for 16 hours at desired temperatures, and then removed and sealed in plastic container with some water added to maintain 100% relative humidity and left to equilibrate for a day at relevant temperature ($20\,^{\circ}$C or $60\,^{\circ}$C), before measurements were made at room temperature. The two and four probe setups are as illustrated in the schematic Figure 2 below.

A similar procedure has been used for preparing sample for the two probe method as for the four probe method; however samples larger than the 1.18 cm^2 probe surface were sandwiched between the graphite paper to allow for good equilibration. The value of the real intercept in the Imaginary vs. real impedance plot (Bode plot) in the high frequency range is taken as the bulk resistance of the membrane. This is used in the expression below to calculate ion conductivity.

$$\sigma = \frac{l}{RA} \tag{3}$$

Where σ is the conductivity in (Siemens, S/cm), l is the distance between electrodes in cm (counter and working electrodes in the 4-probe method), R is the bulk resistance (Ω), and A is the membrane area normal to ion flux (cm^2).

Results and Discussion

Membranes were cast in this study with the intent of kinetically trapping a random but phase separated morphology. This has been shown in previous block copolymer studies to decrease the effective tortuosity, and hence shorten the diffusion path length of the domain through which the species being transported permeates the membrane, resulting in improve transport properties[21]. In block copolymer ionomer systems the use of a mixture of polar and nonpolar solvents have been shown to produce a more random phase separated microstrucure which also had the effect of increasing permeability across the membrane [13,22], due to an enhanced connectivity of domains which provide more favorable diffusion of penetrant across the membrane[12]. With the careful choice of the other block(s) to disallow diffusion of fluid, this can serve the purpose of maintaining mechanical integrity of the material especially in cases where transport of fluid is dependent on water content.

To this end a mixed solvent pair was chosen comprising toluene, which is a good solvent for FISS neutral copolymer, and NMF a highly polar cosolvent which will solvate the ionic domains in all the samples, especially the cesium neutralized samples. Also to varying degrees, this solvation is accomplished by dissociation of the counterions, which upon drying are available to frustrate the formation of regular equilibrium block copolymer morphologies due to presence of strong columbic interactions which lead to aggregation in the ionic domains.

Block copolymer systems have been well studied and exhibit a rich diversity of morphologies which include the classical spherical, cylindrical and lamellar morphologies, as well as the gyroid[23]. These morphological forms are brought about by the process of self assembly into separated phases, which is governed by the degree of dissimilarity in the adjacent blocks, as well as the volume fraction of each block. It is usually observed by means of small angle x-ray scattering (SAXS) or TEM, with feature sizes ranging from 5 to 50nm[24]. The figures 3 below shows TEM images of the membrane samples prepared.

The dark parts of all images represent the partially sulfonated domains. Solid thick dark lines in the images represent gold used as a marker at the surface of the membrane, so a normal to this gold line in the direction of the film represents its depth. As was desired we observe a disordered morphology having sulfonated PS domains interconnected to essentially the same degree in the AC50,AC28 and CS23 samples. These grainy structures represent cylinders of partially sulfonated PS domains in a fluorinated PI matrix. A hexagonally packed cylindrical morphology is typically observed in unsulfonated PS-PI diblock copolymer with same volume fraction of PS as the precursor material (27mol% of PS). However as reported in other block copolymer ionomer studies there is a reduction in long range order upon addition of ionic groups[22,25]. These disordered cylindrical domains can be seen to impinge on one another in the images, this will lead to a degree of interconnectivity in the transporting phase. Upon swelling in water and/or methanol this is expected to be further enhanced under fuel cell operating conditions, leading to a network proton conducting channels across the

thickness of the membrane. This structural evolution has been shown in other copolymer ionomer studies[4,26], and is the subject of a subsequent publication[27].

The CS50 sample however, shows a lamella morphology with domains aligned parallel to the film surface. The reason for the formation of this classical neutral block copolymer morphology is not fully understood, however when the choice of the polar cosolvent was being made, it was observed that this sample was the most difficult to dissolve. n-butanol and DMSO were tried but could not dissolve this sample, necessitating the use of NMF in this and all other samples for consistency. The cosolvents listed above are in order of increasing dielectric constant , which is an indirect measure of their ability to dissociated the counterion from the sulfonic acid group and hence dissolve the ionomer. With the foregoing it is safe to assume that this sample had the least amount of counterion dissociation (due to the larger quantity of Cs ions in the ionic domain), and hence there was minimal interference to the normal block copolymer self assembly process by free counter ions. This may also have to do with the low affinity of Cesium for polar solvents.

Self-assembly in block copolymer ionomers have consistently shown ordering at two length scales, due to the neutral block copolymer phase separation and ionic cluster formation[28,29]. To capture the sizes of the different structural features (domains or ionic clusters) in this hierarchical microstructure, different configurations of SAXS cameras are typically used for the different q ranges; however we have been able to use a USAXS camera to capture several decades at one shot.

The characteristic dimension of the scattering objects can be obtained by substituting the value q* of the first-order peak from the scattering intensity versus scattering vector plot I(q) versus q), into the Bragg law given by the expression:

$$d = \frac{2\pi}{q^*} \qquad (4)$$

This bragg spacing represents the average center-to-center distance between scatterers. In scattering profiles of samples with more regular spatial arrangement , the higher order peaks are visible, and the type of structures packed on the lattice can be determined using the ratio of higher-order peaks to the first-order peak (q^i/q^*). A profile with hexagonally packed cylinders would therefore have a relative peak ration of $1, \sqrt{3}, 2, \sqrt{7}$ …, while a lamellar morphology, would have a ratio of 1,2,3,4 ….[30]. The inter-aggregate distance in the ionic domains can also be calculated by using the ionomer peak position in the Bragg equation. These will be found in a separate phase embedded in the PS domains which are in turn phase separated from the fluorinated PI domains[31]. The slit desmeared USAXS profiles from the membrane samples studied are shown in Figure 4 below

We observed a prominent peak in both the AC28 and the CS23 samples at a position q= 0.030861 A[-1]. This corresponds to a characteristic dimension of 20.3 nm for both samples. A faint peak at q = 0.052879 A[-1] can be seen in the profile for the CS23, and this would have a q^i/q^* ratio of 1:1.71, which is approximately representative of hexagonally packed cylinders(q^i/q^* ratio of 1:1.73). Combining this information with the TEM images obtained we can deduce that these two samples have a morphology

composed of cylinders arranged imperfectly on a hexagonal lattice. Since the SAXS beam went into the membrane normal to the surface and there is a slight secondary peak in the CS23 sample, there is evidence of some cylinders oriented perpendicular to the film surface. It is worthwhile noting that there is no difference in the peak position for both samples. This is due to the fact the molecular weights of both samples are similar and so are their styrene weight fractions.

We also observe at a smaller length scale a broad peak in both samples with peak position centered around $q = 0.13264$ A^{-1} which corresponds to a bragg spacing of 4.7 nm. This is known as the ionomer peak, which represents the ionic clusters or aggregates. The intensity of this peak is greater in the cesium sample, as expected, due to the higher X-ray contrast relative to the acid samples.

In the CS50 sample we observed a similar hierarchical structure with the first order peak position at $q= 0.026455$ A^{-1}, corresponding to a bragg spacing of 23.7nm. Two other peaks were visible at $q= 0.052876$ A^{-1} and $q= 0.077556$ A^{-1}, which yield a $q^i/q*$ ratio of 1:1.99:2.93. This confirms the lamellar morphology observed in the TEM image and suggests that the lamellae sheets lie predominantly in a direction normal to the membrane surface. For both this sample and the AC28/CS23 samples, there is evidence of mixed or random orientation of the domains as the orientation evident in the TEM images are opposite to that in the SAXS. However SAXS information gives a better average of the existing morphology.

We also observe an ionomer peak for this sample within approximately the same q range as seen for the other samples however, the peak is centered at a position yielding a bragg spacing of 3.2nm. It is not clear as to why this sample has a smaller ionic characteristic dimension, however it is safe to assume that with an increased sulfonation there will be a greater crowding of aggregates in a similarly sized block domain, leading to shorter center-to-center distances. We collected USAXS data down to $q=0.0001$ A^{-1} for all samples. The general trend shows an $I\sim q^{-d}$ dependence, where $2 << d < 3$ for AC28, CS23 and CS50 samples, suggesting a self-similar mass fractal structure[32]. However the AC50 sample has a power law slope of -3.5 suggesting a rough surface fractal structure. This sample also shows a weak peak at a bragg spacing around $q= 0.027679$ A^{-1}, yielding a brag spacing around 22.7 nm. This peak represents the block copolymer characteristic dimensions. The ionomer peak was however indistinguishable.

The transport properties of the investigated membranes are summarized in table 2.1 below. Data from Nafion[TM] 112 of similar thickness are also included for comparison. All experiments have been done under the same conditions.

The water uptake data show an increase in uptake both for increasing level of sulfonation as well as for increasing temperature. For the samples with the cesium counterion the water uptake measured is relatively lower than their acid counterpart. This is similar to results for Cs+ ion doped Nafion[TM] reported by Tricoli[14]. Cesium ions are known to have less affinity for water, due to their lower hydration energy[33]. This may however be dependent on other factors such as membrane morphology, and glass

transition of the material. The CS50 sample disintegrate upon soaking in water at 60°C, whereas the AC50 sample does not. With lamellae layers lying perpendicular to the membrane surface the CS50 samples can be more easily pried apart upon swelling. The AC50 samples also swell markedly by 595% upon soaking in water at 60°C and are softened significantly. The results shown are an average of two samples per polymer.

Methanol permeation through our FISS and Nafion[TM] membrane samples were measured by the method earlier described , and the specific concentration of permeated methanol in the receiving chamber has been plotted as a function of time in Figure 5. The slope of these graphs in the linear regions, yield the permeability of methanol through the membrane and have also been summarized in table 2.1. For samples prepared at 20°C we observe an order of magnitude less methanol permeability for the AC50 sample compared to Nafion[TM] 112, however the result for the CS50 sample is just a little less. This may reflect the difference in morphologies of these two FISS samples. These values measured are similar to those reported for other styrene based ionomers[13,18,34].

No methanol cross-over could be detected for the AC28 and CS23 samples. However at 60°C these samples showed 27 times less permeability than Nafion[TM] 112. The higher sulfonation membranes could not be measured at this temperature as they had swollen excessively and suffered mechanical failure under the osmotic pressure exerted by the 2M methanol solution.

Proton conductivity has been measured both in the plane and normal to the plane of our membrane samples, using the four-probe and two-probe methods respectively. The two methods should ideally give the same result, since the ions are moving through the same membrane, however there is a significant impedance contribution by the interface at low frequencies[20]. For the application of block copolymer ionomers to DMFC technology, the more relevant measurement is that taken normal (across) the plane of the membrane as the methanol flux in a functioning fuel cell is in that direction. Also block copolymer domains may possess some orientation which will impact the transport of ions the conducting phase. For these and other reasons the conductivity values measured using the two probe method are typically less than for the Four point probe[35] . The conductivity values obtained have also been summarized in table 2.1 and are represented in Figure 6 below.

The conductivity values for Nafion 112[TM] were measured for comparison with the FISS samples and published work in literature. Though most of the literature reports for Nafion conductivity measurements have been made using thicker Nafion 117[TM] , however one study using the 50 micron thick Nafion 112[TM] has reported an in-plane conductivity of 0.06 S/cm[36] at 80°C, whereas this study reports 0.065 S/cm at 60°C. The conductivity values measured with this geometry at room temperature for our AC50 and CS50 materials are about the same at 0.0011S/cm and 0.0013 S/cm respectively. The CS50 samples has a higher conductivity under these conditions possibly due to the lamellar morphology lying perpendicular to the film surface. The conductivity value measure at 60°C are higher for both Nafion 112[TM] and AC50 due to greater chain mobility at higher temperature, and higher water uptake which facilitates proton transport.

The ionic conductivity measured in this geometry for both the AC50 and CS 50 samples are less than that for Nafion 112[TM] by more than an order of magnitude. In like manner, the conductivity of other styrenic copolymer ionomers have been reported to be less than Nafion,[18,26] depending on the degree of sulfonation, as well as the morphology of the copolymer. This can also be attributed to the fact that the fluorosulfonic acid found in nafion is a stronger acid than the styrene sulfonic acid in the styrenic systems. This deficit in conductivity can usually be made up for by increased sulfonation, but usually at the cost of softening due to increased swelling. Some sulfonated aromatic polymers having significantly more chain stiffness have however been able to bear more sulfonic acid groups with minimal swelling[3].

For the two probe conductivity measurement which measures ionic conductivity across(through) the plane of the membrane, we see more than an order of magnitude less conductivity for all the samples with respect to the four probe method. This is mainly due to the difference in the experimental setup as this configuration has a much higher electrode surface area than the four probe configuration, and also there is charge buildup at the membrane-electrode interface leading to increased effective resistance[37,38]. This typically leads to lower conductivity values [35]. For the samples soaked at 60°C AC50, the in-plane conductivity is 48 times less than nafion112 whereas the, through plane conductivity of AC50 is only 2 times less than Nafion112. Since the through plane measurements are more relevant to a functional fuel cell, and both materials were measured in the same way these values are more descriptive of the actual membrane conductivity in a fuel cell.

The AC28 and CS23 samples did not show any measurable conductivity values. This is possibly due to the sulfonic acid concentration being less than the percolation threshold for these materials, or their low water uptake. Also for these samples with low sulfonation the fluorinated phase will tend to have less competition in migrating to the surface layer as they have a lower surface energy than the sulfonated phase, leading to interfaces with reduced surface tension which is preferred. In order to test this hypothesis, an atomic force microscopy (AFM) study of the membrane surfaces was carried out. The scan from the smoother surface of each membrane adjoining the neutralized glass plate are shown in the Figure 7 below.

The darker domains in the contrast image on the right represent the fluorinated phase which is softer. In the AC28 and CS23 images there is an almost uniform dark phase, which signifies the presence of a surface layer of mainly the fluorinated phase. This can explain the non-detectable ionic conductivity or methanol permeability of these samples, since the phase that allows permeation would have to be present on each surface and be connected from one surface of the membrane to the other.

However in the images for the AC50 and CS50 samples with higher sulfonation levels there is evidence of both a lighter and a darker phase at the surface. As seen in the TEM images for these samples the AC50 sample has a speckled morphology with spots of the lighter domain (sulfonated PS, and PS) will dispersed in the darker domain, where

as the CS50 sample shows stripes of both light and dark domains running diagonally across the surface resembling a lamellar morphology. These surface morphologies with the hydrophilic phase present in greater amount, would favor higher ionic conductivity to the surface as is the case from our conductivity results.

Conclusions

New proton conducting membranes have been developed based on partially sulfonated poly(Styrene)-block- fluorinated poly(Isoprene). A randomly microphase separated morphology has been achieved using mixed polar and non-polar solvents, and USAXS has been used to elucidate the hierarchical structure and fractal dimensions which are favorable for enhanced transport properties. Low methanol permeability has been recorded relative to Nafion 112^{TM}, however modest proton conductivity values were obtained. We believe that with further crosslinking of the residual polystyrene units to reduce swelling and optimization of the casting process, promising inexpensive candidates for low temperature direct methanol fuel cells will emerge.

References

(1)   O'Hayre, R. P.; Cha, S.; Cololla, W.; Prinz, F.B. In *Fuel Cell Fundamentals* ; 1 ed.; John Wiley& Sons, Inc: New York ,**2006**; p 12.

(2)   Arico, A.S.; Srinivasan, S.; Antonucci, V. *Fuel Cells* **2001**,1,133.

(3)   Hickner, M. A.; Ghassemi, H.; Kim, Y. S.; Einsla, B.R.; McGrath, J. E. *Chemical Reviews* ,**2004**, 104,.4587.

(4)   Gierke, T.D.; Munn, G.E.; Wilson, F.C. *J. Polymer Sci: Polym. Phys. Ed.* **1981**, 19, 1687.

(5)   Yang, Y.; Holdcroft, S. *Fuel Cells* **2005**, 5,171.

(6)   Bishop, M.T.; Karasz, F.E.; Russo, P.S.; Langley, K.H. *Macromolecules* **1985** ,18, 86.

(7)   Wainright, J. S.; Wang, J.T.; Weng, D.; Savinell, R.F.; Litt, M.J. *J. Electrochem. Soc.* **1995**,142, L121.

(8)   Miyatake, K.; Hay, A. S. J. *Polym. Sci., Part A: Polym. Chem* **2001**, 39, 3770.

(9)   Savett, S.C.; Atkins, J.R.; Sides, C.R.; Harris, J.L.; Thomas, B.H.; Creager, S.E.; Pennington, W.T.; DesMarteau, D.D. *J. Electrochem. Soc.* **2002**,149, A 1527.

(10)   Kim, Y.S.; Wang, F.; Hickner, M.; Zawodzinski, T. A.; McGrath, J.E. *J. Membr. Sci.*, **2003**, 212,263.

(11)   Herz, H.G.; Kreuer, K.D.; Maier, J.; Scharfenberger, G.; Schuster, M.F.; Meyer, W.H. *Electrochim. Acta* **2003**, 48,2165.

(12)   Gido, S.P. In *ACS Symposium series: New Polymeric Materials* **2005**, 916,309.
(13)   Kim, B.; Kim, J.; Jung, B. *J. of Membrane Science* **2005**, 250,175.
(14)   Tricoli, V. *J. Electrochem. Soc.* **1998,** 145, 3798.
(15)   Huang ,T.; Gido, S.P.; Mays, J.W. *Synthesis and Characterization of Fluorinated and Sulfonated Block Copolymers for Fuel Cell Proton Exchange Membrane*, Unpublished manuscript.

(16)   Miyake, N.; Wainright, J.S.; Savinell, R.F. *J. Eletrochem. Soc.* **2001**, 148, A898.
(17)   Long, G.G.; Allen, A.J.; Ilavsky, J.; Jemian, P.R.; Zschack, P. In *Synchrotron Radiation Instrumentation: Eleventh US National Conference*, CP521, Pianetta, P.; Winick, H. Eds.; , American Institute of Physics, College Park, 2000, pp. 183–187.

(18)   Elabd, Y. A.; Napadensky, E.; Sloan, J. M.; Crawford, D.M.; Walker, C.W. *J. Membr. Sci.* **2003**, 217, 227.

(19)   Crank, J. *The Mathematics of Diffusion*; Oxford University Press: Oxford, 1975.
(20)   Cahan, B.D.; Wainright, J.S. *J. Electrochem. Soc.* **1993**, 140, L185.
(21)   Drzal, P.L.; Halasa, A.F.; Kofinas, P. *Polymer* **2000**, 41, 4671.
(22)   Elabd, Y. A.; Napadensky, E.; Walker, C. W.; Winey, K. I. *Macromolecules* **2006**, 39, 399.

(23)   Bates, F. S. *Science* **1991**, 251, 898.
(24)   Bucknall, D.G.; Anderson, H.L. *Science* **2003**, 302,1904.
(25)   Storey, R.F.; Baugh III, D.W. *Polymer* **2000,** 41, 3205.
(26)   Serpico, J.M; Ehrenberg, S.G; Fontanella, J.J.; Jiao, X. Perahia, D.; McGrady, K.A.; Sanders, E.H.; Kellogg, G. E.; Wnek, G. E. *Macromolecules* **2002**, 35,5916.

(27)   Isaacs-Sodeye A. I.; Huang T.; Mays J.; Gido S. P. "Block copolymer ionomers from Fluorinated Poly(Isoprene)-*block*-Sulfonated Poly(Styrene) 2: Structural evolution with swelling and in solution" *Manuscript in Preparation.*

(28)   Williams, C.E.; Russell, T.P.; Jerome, R.; Horrion, J. *Macromolecules* **1986,** 18, 2877.

(29)   Lu, X.; Steckle, W.P. Weiss, R.A. *Macromolecules* **1993** 26, 5876.
(30)   Sakurai, S.; Momii, T; Taie, K.; Shibayama, M.; Nomura, S.; Hashimoto, T. *Macromolecules* **1993**, 26, 485.

(31)   Yarusso, D.J.; Cooper, S. L. *Macromolecules* **1983**,16,1871.
(32)   Roe, R. *Methods of X-Ray and Neutron Scattering in Polymer Science*; Oxford University Press: New York, 2000; p189.

(33)   Cotton, F.A.; Wilkinson, G. *Advanced Inorganic Chemistry*, John Wiley: New York, 1972, p 645.

(34)   Carretta, N.; Tricoli, V.; Picchioni, F. J. *J. Membr. Sci.* **2000**, 166, 189.

(35)   Deluca, N. W.; Elabd, Y. A. J. *Polym. Sci., Part B: Polym. Phys.* **2006**, 44, 2201.

(36)   Swier, S.; Chun, Y.S.; Gasa, J.; Shaw, M.T.; Weiss, R.A. *Polymer Eng. Sci.* **2005**, 45,1081.

(37)   Pivovar, B.S.; Wang, Y.; cussler, E.L. *J. Membr. Sci.* **1999**, 154, 155.

(38)   Alberti, G.; Constantino, U.; Casciola, M.; Ferroni, S.; Massinelli, L.; Staiti, P. *Solid State Ionics* **2001**,145, 249.

Table 1 Thickness, Water uptake, methanol permeability and ionic conductivity of materials investigated in this work.

Polymer	Dry Thickness (υm)	Water Uptake (%)		Methanol Permeability (cm^2/s)		In Plane Conductivity (S/cm)		Across Plane Conductivity (S/cm)	
		$20^{o}C^{b}$	$60^{o}C^{b}$	$20^{o}C$	$60^{o}C$	$20^{o}C^{b}$	$60^{o}C^{b}$	$20^{o}C^{b}$	$60^{o}C^{b}$
Nafion 112	50			2.6×10^{-7}	25.4×10^{-7}	1.82×10^{-2}	6.45×10^{-2}	8.47×10^{-5}	3.51×10^{-4}
AC50	81	17	595	2.0×10^{-8}	a	1.06×10^{-3}	1.33×10^{-3}	5.38×10^{-6}	1.57×10^{-4}
CS50	91	5	a	2.4×10^{-7}	a	1.26×10^{-3}	a	4.24×10^{-6}	a
AC28	69	5.4	257	0	2.0×10^{-8}	a	a	a	a
CS23	74	2.4	129	0	2.0×10^{-8}	a	a	a	a

[a]Not Measurable

[b]Processing Temperature
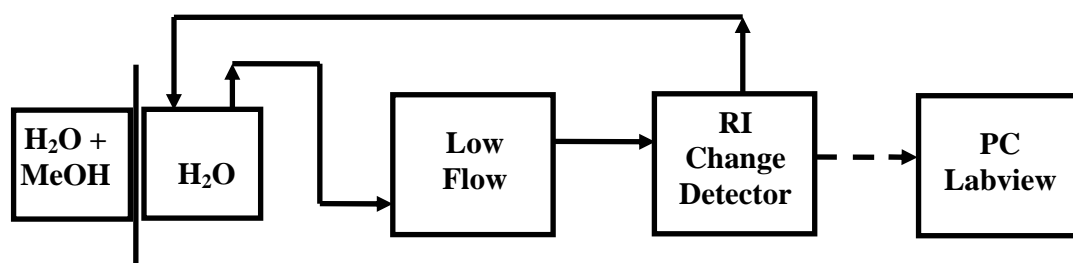
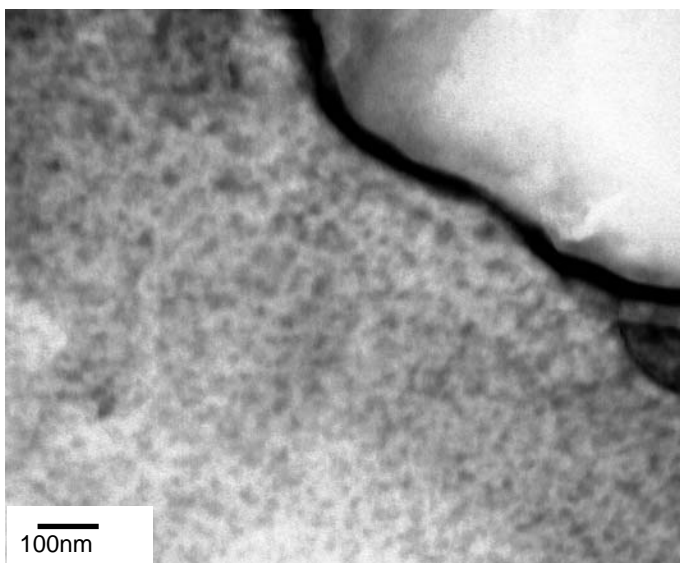Figure 1   Flow diagram and pictures of Methanol Permeability measurement Experimental Setup.
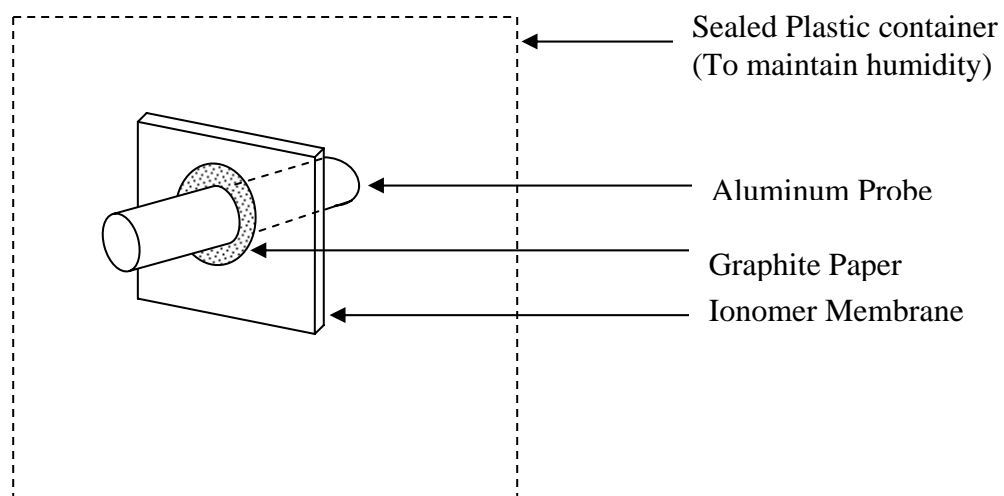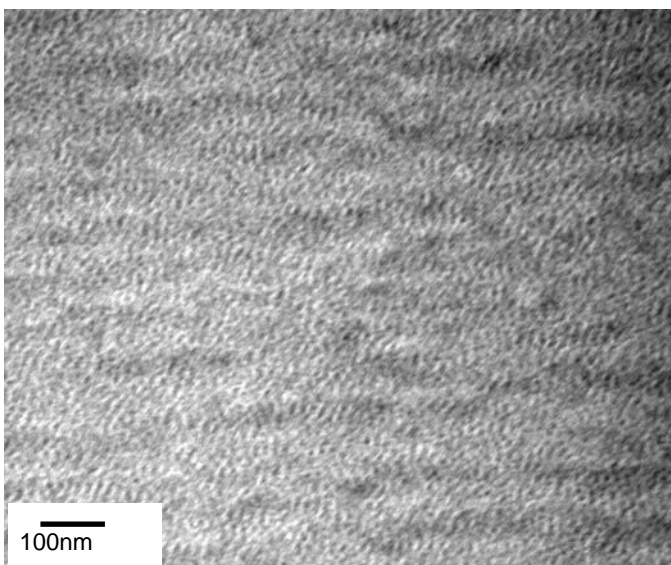
(a)
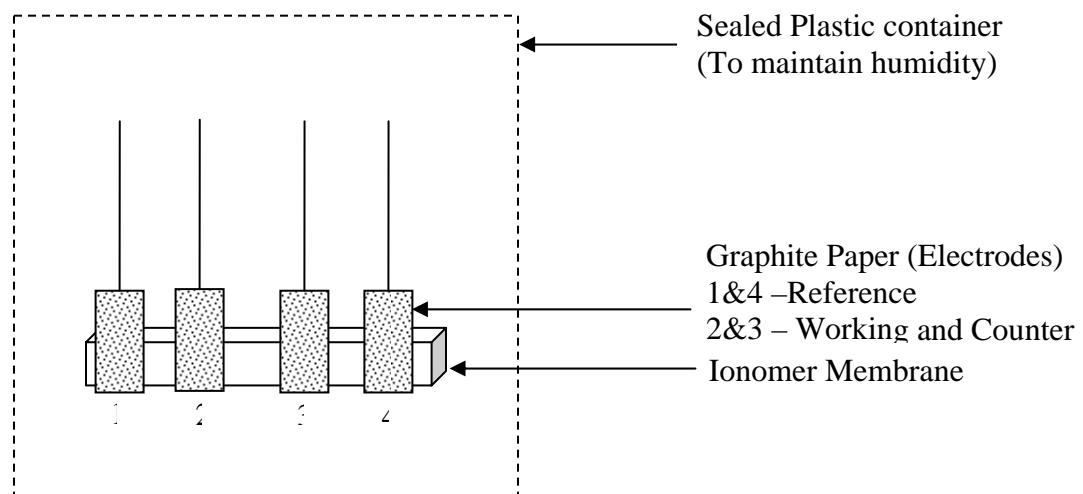
(b)

Figure 2 Experimental Setup for a) Two Probe , b) Four Probe EIS measurements.

AC28

AC50

Figure 3   Transmission electron Microscopy images for the FISS samples. (Continued)
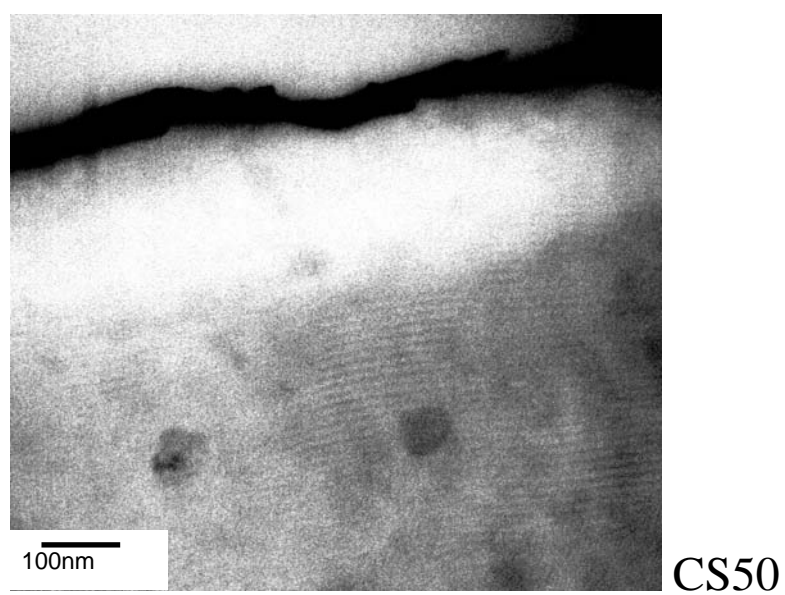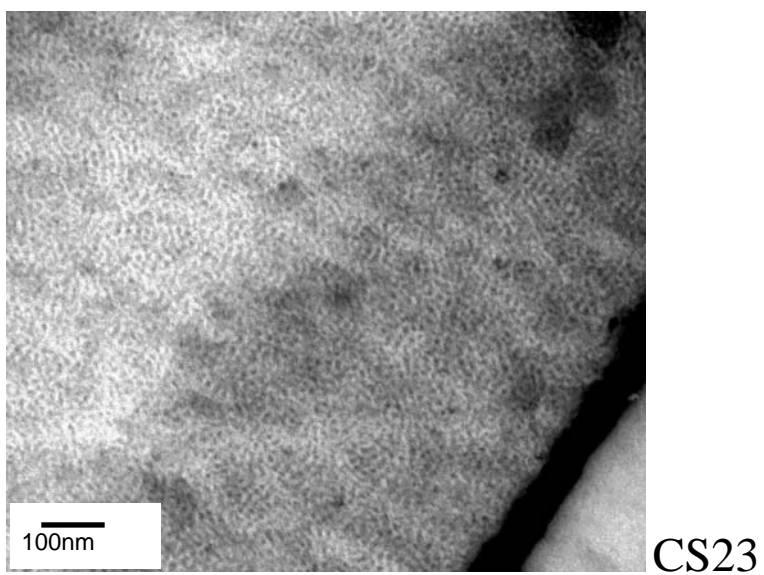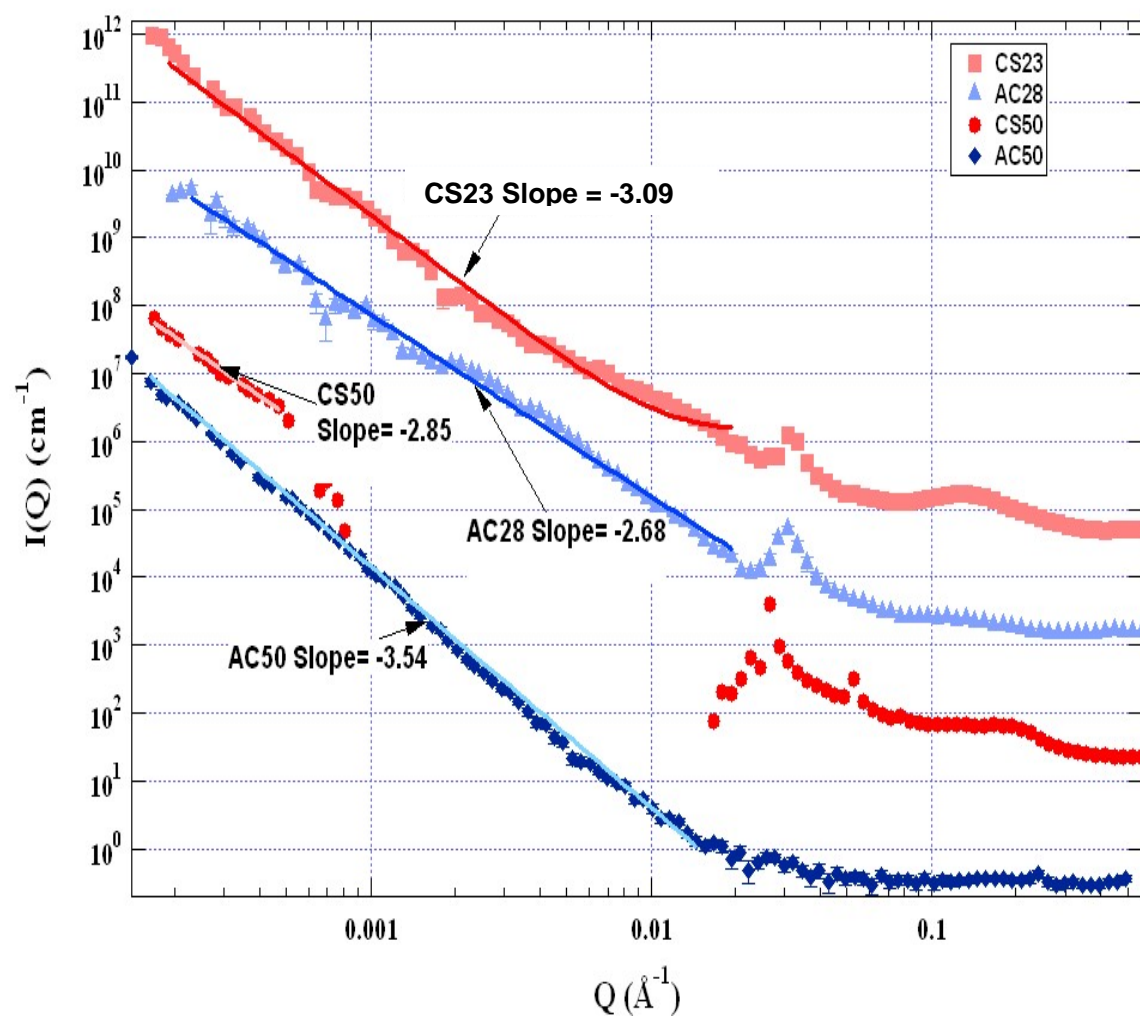
CS23

CS50

Figure 3   (Continued)

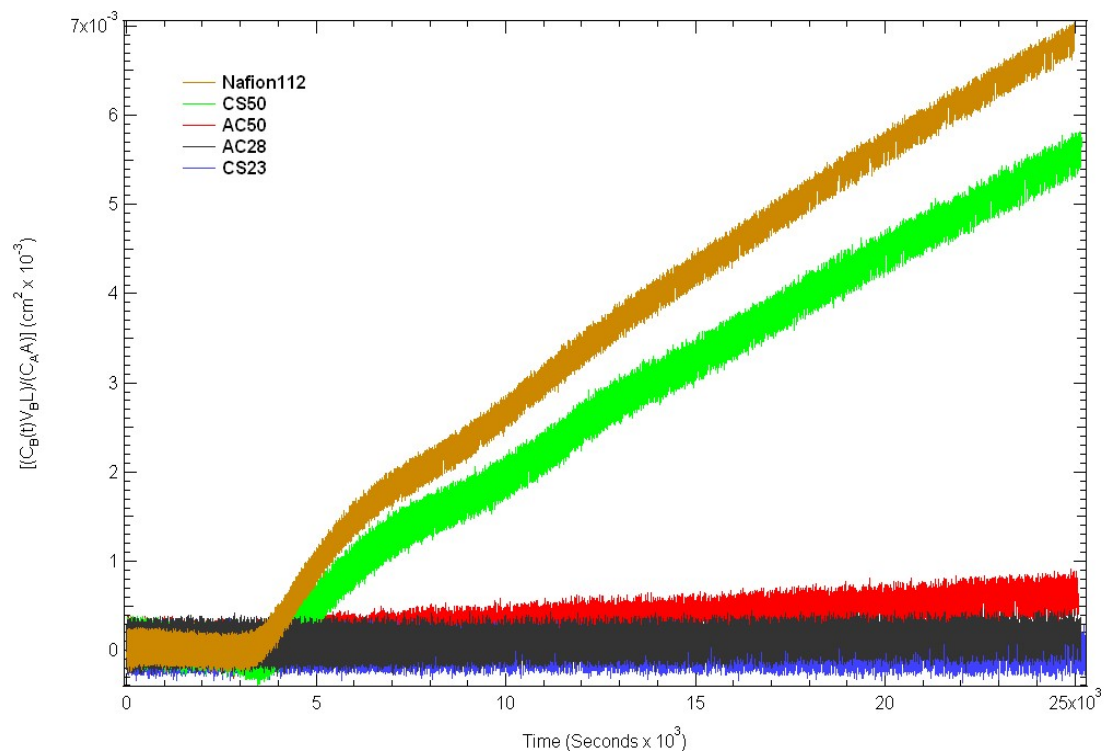Figure 4   Ultra Small Angle Scattering Profiles for the FISS samples.
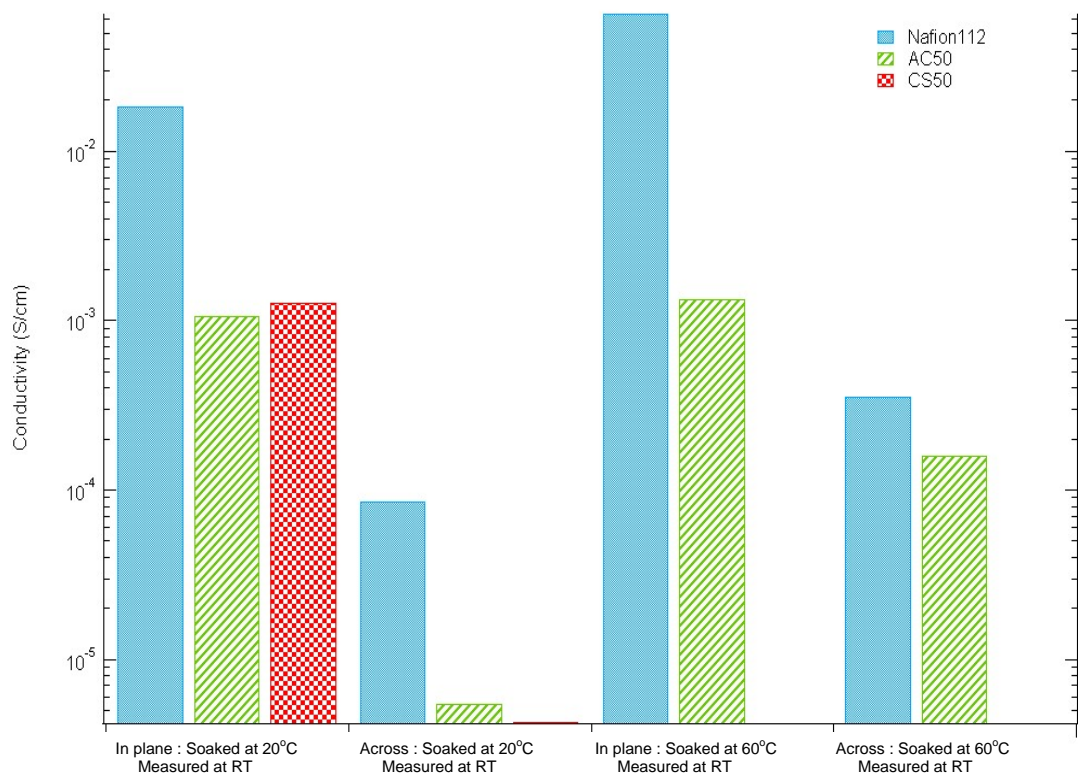
Figure 5   Specific concentration of permeated methanol versus Time measured at 20°C.
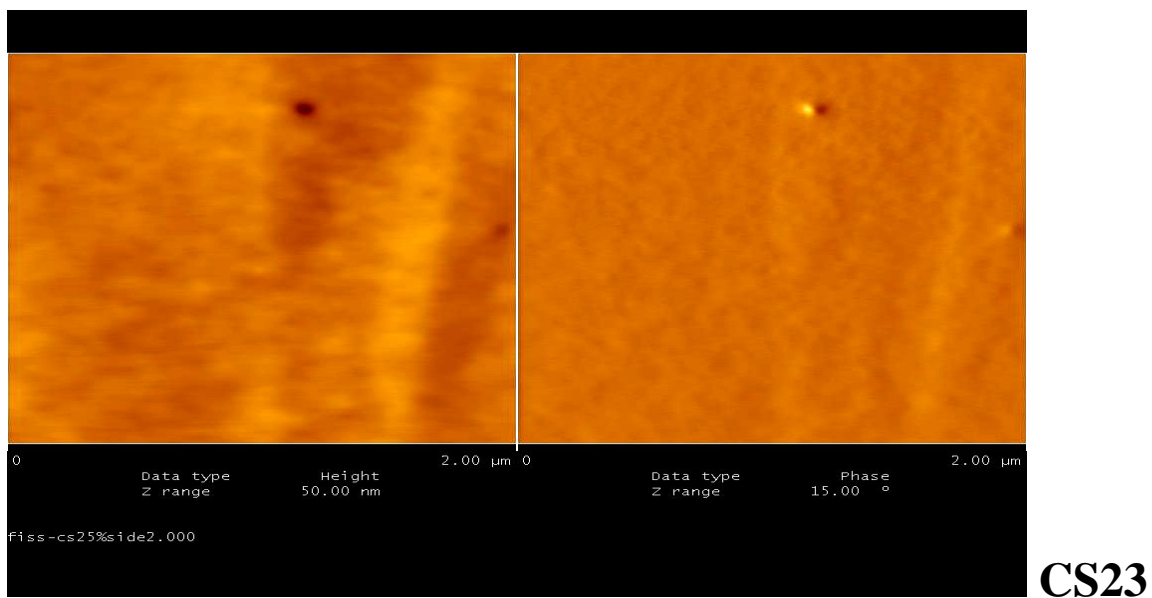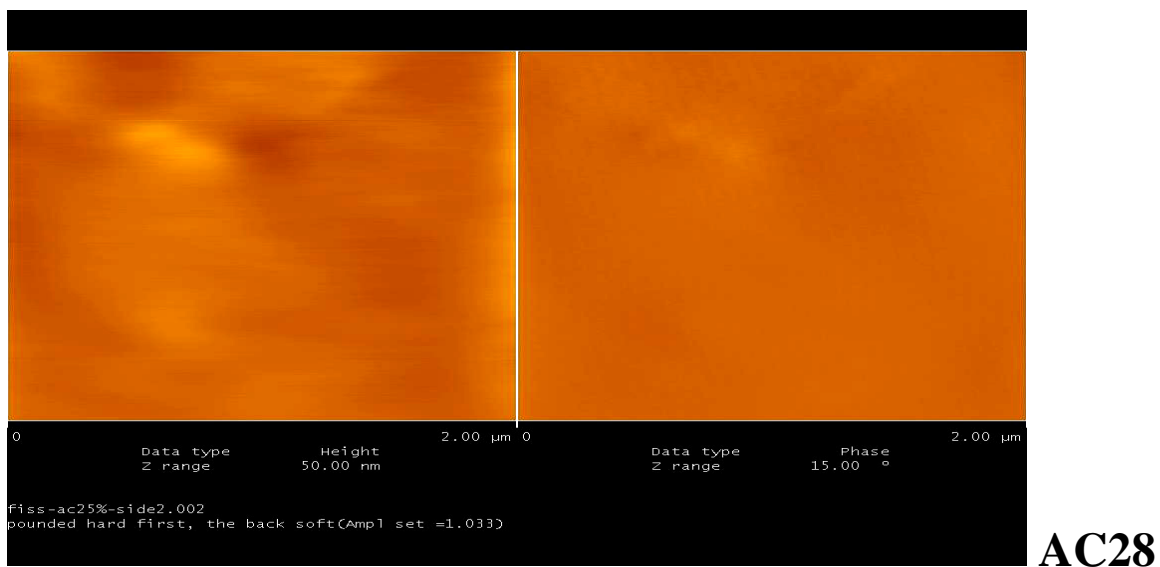
Figure 6　　　Ionic Conductivity of measurable samples.

Figure 7 AFM images of membrane surface adjacent to casting glass plane. (Continued)
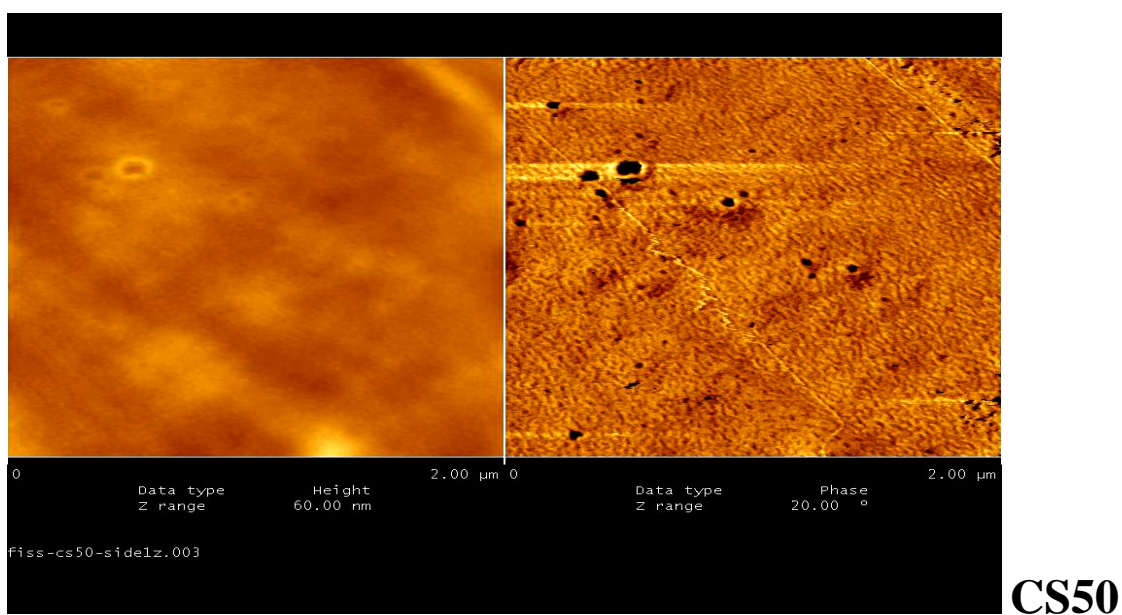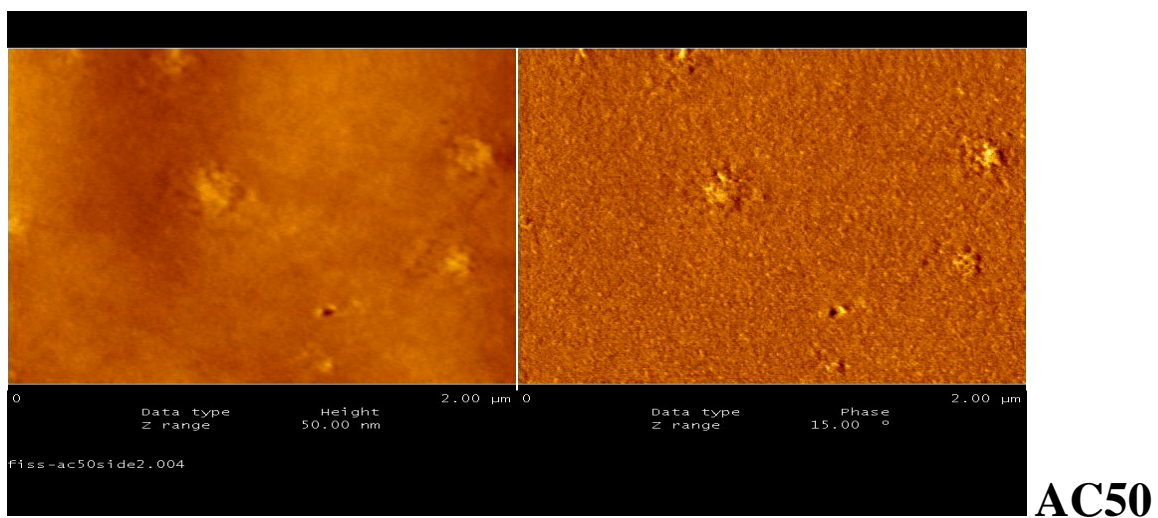
AC50

CS50

Figure 7 (Continued)

(5.2) POLYMER ELECTROLYTE MEMBRANES FROM FLUORINATED POLY(ISOPRENE)-BLOCK-SULFONATED POLY(STYRENE): STRUCTURAL EVOLUTION WITH HYDRATION AND HEATING

Abstract

SANS and USAXS have been used to study the structural evolution of FISS materials as they have evolved from the dry state to the water swollen state. A dilation of the nanometer-scale hydrophilic domains has been observed as hydration increased , with greater dilation occurring in the higher sulfonated sample or upon hydration at higher temperatures. Furthermore a decrease in the order in the these phase separated structures is reduced upon swelling. The glass transition temperature of the fluorinated blocks have been seen to decrease upon hydration of these materials, and at the highest hydration levels , DSC has shown the presence of tightly bound water. A precipitous drop in the mechanical integrity of the AC50 materials is also observed upon exceeding the Tg as measured by DMTA. Finally, highly sulfonated CS97 samples have shown the formation of spherical micelles , even at concentrations as low as 0.05 mg/ml. This is related to the great dissimilarity of the blocks (fluoropolymer versus ionic) in these ionomers. The sizes of these micelles range from 13-13.5 nm, with the higher concentration solutions having smaller radius of gyration , possibly due to crowding effects.

Introduction

The study of the structure of ionomers under conditions at which they will be used can shed light on the observed properties of such materials. Ionomers have increasing utility in various areas of research and industry such as batteries, fuel cells, electrolysis cells, ion exchange membranes, sensors, electrochemical capacitors, modified electrodes and even golf balls[1].

Ionomers typically are comprised of a hydrophillic acid bearing phase embedded in a hydrophobic phase. The hydrophillic phases are known to form due to aggregates of the acid groups in to multiplets or larger clusters[2-4]. Nafion[TM] which is the most used ionomer material in PEM applications, is composed of a hydrophobic fluoropolymer backbone and hydrophilic fluorosulfonic acid bearing side chains[5]. Other materials range from fluoropolymer to aromatic to hydrocarbon backboned materials, bearing pendant acid groups in one configuration or another[6].

The clusters formed by the acid groups at the end of the side chains are essential in facilitating ionic conductivity by absorbing water which dissociates the proton counter

ions, forming a hydronium ions which in turn hop from one acid site to the next during transport[7]. Thus the quantity, shape, size, and connectivity of these ionic aggregates dictate the observed transport properties of such materials.

When block copolymers of these ionomers are made , typically in the diblock ,triblock or graft copolymer architectures[8], an extra level of morphological complexity is introduced which yields a hierarchical structure. As in normal block copolymers, nanometer scale phase separation occurs between the blocks, creating separate hydrophobic and hydrophilic domains with morphologies similar to neutral block copolymers. The acid groups in the hydrophilic domains further form clusters at a smaller length scale[9,10].

Swelling or dilation of ionomers upon increasing water or methanol content, and at service temperatures is also an important factor affecting conductivity and mechanical integrity. Block copolymer ionomers with one block being a fluoropolymer have been shown to exhibit enhanced network formation and mechanical integrity especially when hydrated[11]. Backbone stiffness and counterions attached to the acid sites are known to affect the degree of water uptake and hence, swelling[6,12]. The structure of Nafion[TM] has been shown to undergo evolution and phase inversion in order to conserve specific surface as water content increases[13].

With a view to understanding of the swelling induced structural evolution of our fluorinated poly(Isoprene*)-block-*sulfonated poly(Styrene) ionomers from the dry membrane to solution, we have investigated its structure using USAXS and SANS under conditions mimicking fuel cell usage. Furthermore we have looked at the state of water in these systems, and the effect of swelling on thermal transitions using differential scanning calorimetry (DSC),. Finally the thermal and mechanical transitions were studied using dynamic mechanical thermal analysis (DMTA).

Experimental Section
Materials
The synthetic procedures and characterization for fluorinated poly(Isoprene*)-block-*sulfonated poly(Styrene) (FISS) materials have been described in detail elsewhere[14]. The precursor poly(styrene)-block- poly(Isoprene) (PS-PI) diblock copolymer used in this work was anionically polymerized, having reported characteristics: Mw =31,200 ,PDI=1.05, 27mol% PS. The fluorinated samples cast into membranes were sulfonated to 23,28 and 50 mol%, as determined by ^{1}H NMR. Some of these samples were neutralized to the cesium salt form , and the balance left in the acid form. The cesium form facilitates contrast in the X-ray scattering experiments, besides exhibiting different transport properties. Nafion[TM] 112 was generously donated by Atofina Chemicals Inc., and was pretreated to the acid form according to the procedure reported elsewhere[15]. Another PS-PI diblock copolymer having Mw= 32,700, PDI 1.01 , 52mol% PS; was fluorinated and sulfonation to 97mol% for use in micellization studies in aqueous media. A sample coded FISS-AC50 would refer to the acid form of the material, sulfonated to 50mol% of the styrene units in the PS block.

Preparation of Membranes

Freeze dried FISS samples were dissolved in a mixture of toluene/N-methylformamide(THF/NMF:85/15 (w/w)) with a concentration ranging from 12-15 wt%. The NMF was used as a polar cosolvent. These solutions were then cast unto glass plates for a day in the fume hood at room temperature for rapid casting of kinetically trapped disordered morphology. Subsequently they were placed in an oven for 1 day at 60^oC , and finally in the oven at 60^oC under vacuum for a day to remove most of the residual solvent. The acid-form samples were further reactivated by soaking overnight in a 2M aqueous HCL solution containing methanol (20v/v) to enhance swelling and acid permeation. They were thereafter rinsed repeatedly in deionized water till PH was neutralized and then dried at 60^oC in a vacuum oven for a day, and again in vacuum plus 60^oC for one day. Cast membranes were subsequently removed and stored in airtight bags for further usage. Dry membrane thicknesses were measured using a digital micrometer and range from 60-90 υm. The Nafion 112 samples were also rinsed until PH was neutral, then dried at 60^oC in a vacuum oven for a day and stored in the same way.

Structural Characterization

Small angle x-ray scattering(SAXS) was performed at the Advanced Photon Source(APS) in Argonne National Laboratory on beamline 32-ID, fitted with a Bonse-Hart camera typically used for ultra small angle x-ray scattering (USAXS), which has been described elsewhere. The x-ray energies range from 7 to 18 keV, yielding a q range from 0.0001 to 1.0 A^{-1} (where q, the scattering vector is equal to $4\pi\sin(\theta)/\lambda$, where 2θ is the scattering angle and λ is the wavelength of the incident radiation). The beam size was 1mm x 2mm, and a 1-dimensional photodiode detector was used. Air-blanks were subtracted and slit desmearing of the resulting data was carried out using the lake method. All SAXS data were collected with the samples in the transmission position, with membrane normal in the direction of the beam.

Small angle neutron scattering (SANS) experiments were also carried out on both dry and hydrated samples, at the Intense pulsed Neutron Source (IPNS) at the Argonne National Laboratory. The Small Angle Scattering Instrument (SASI) , having a q range of 0.007 to 1.45 Å^{-1} was used having a q resolution of 0.3 to 0.036. This instrument used an area detector, with area of 50 x 50 cm^2 and 3 - 5 mm (FWHM) detector resolution. The samples were sealed in quartz cells and empty cells were also run for background subtraction.

Samples were hydrated by soaking in D_2O or D_2O vapor for at least 16 hours each at both room temperature (23^oC) and 60^oC. The humidity of the D_2O vapor was controlled by placing jars of appropriate saturated salt solutions of D_2O, having known equilibrium relative humidities[16] into sealed plastic containers, with the membrane samples also placed within the sealed chamber but separate from the solution. A relative humidity and temperature meter was also placed in this chamber before sealing. At the end of the immersion period the hydrated samples were rapidly placed in the quartz cells after blotting of surface D_2O, with the edges sealed using Teflon[TM] tape to prevent

evaporation. These as well as blank cells were placed in the beamline and experimental runs were carried out at room temperature for hydrated membrane samples.

In order to study the self-assembled structure of these ionomers in solution, aqueous solutions of the highly sulfonated samples were made. These samples were dissolved in D_2O with concentration ranging from 0.05 to 10 mg/ml. For the SANS experiments, the solutions were poured into 1 mm thick quartz liquid cells. The lids of these cells were wrapped with teflon tape to prevent evaporation or spillage. These sealed cells as well as cells containing pure D_2O were placed in the neutron beamline at room temperature.

Thermal Characterization

As-received FISS samples were placed in a desiccator over Phosphorus pentoxide for a week in order to dry any absorbed water. They were subsequently placed in an oven at 105^oC overnight under Nitrogen flow. DSC analysis was performed on these dry materials , using a TA Instruments Q200 calorimeter. 4-7mg for samples was placed in aluminum pans, which were sealed in the press. Heating and cooling rate was set to 10^oC min^{-1}. Hydrated membrane samples prepared using water, with the same procedure as described above for SANS measurements, were also sealed in aluminum pans and analyzed.

Dynamic mechanical analyses of the cast FISS membranes were performed with a TA Instruments' DMA 2980, using tensile fixtures. The samples had thicknesses as given in Table 3 below, with length and width of 10mm and 5mm respectively. Heating rate was 3^oC/min , in a temperature range from 25^oC -140^oC, Strain of 15 um amplitude and frequency of 1 Hz. The tensile storage modulus and loss modulus were measured.

Results and Discussion

Structural Evolution with Hydration

The structural evolution of PEM membranes under conditions mimicking use environment is essential to understand the true structure, from which their properties emanate. Specifically the changes in domain sizes as well as the hierarchical structure of the block copolymer ionomers, under varying degrees of hydration and at different temperatures, shed light on the changing transport properties that have been recorded.

In order to determine the center-to-center distance (d spacing) of block copolymer domains and the acid clusters of the FISS samples USAXS experiments were done. The results are summarized below in Table 1. Both the AC28 and CS23 samples have the same block d spacing of 20.3nm and cluster d spacing of 4.7nm. The AC50 and CS50 samples on the other hand have differing d spacing of 22.7nm and 23.7nm respectively. The difference is related to the fact that, though they have the same sulfonation level, they however have different morphologies (see chapter 2) , and hence will have different packing of the chains resulting in different d spacings. The cluster d spacing for the CS50 sample is also less than that for the CS23 sample because of the higher number of clustered acid sites which are more closely packed.

Scattering profiles from these dry FISS samples were also obtained using SANS for comparison and are shown in Figure 1 below. There is a difference in the neutron scattering length density (SLD) between the fluorinated poly(Isoprene) (FI) and the sulfonated poly(Styrene) (SS) blocks. The values for the neutron SLD for both FI and SS block as well as for D_2O are tabulated in Table 2. The contrast between two scattering units is defined as their difference in neutron SLD squared[17]. Using this approach the contrast between D_2O and the FI block gives 0.2423×10^{22} cm^{-4} , while between 50mol % Sulfonated Poly(styrene) and an adjacent FI block gives 0.00065×10^{22} cm^{-4}. The latter contrast though not as great as the former, is sufficient to reveal visible block phase separation peaks, as for some of the other samples.

As can be seen in Figure 1 the CS50 samples have a d spacing of 22.2 nm as compared to 23.7 nm obtained by USAXS. Also the AC28 and CS23 samples have d spacings of 20.2 nm and 19.2 nm, respectively, compared to 20.3 nm measured by USAXS. There is no distinguishable peak for the AC50 sample, which may be due to a diffuse boundary between phases. Only block phase separation peaks can be seen in these SANS spectra, since there is no deuterated water (D_2O) in the clusters. The spectra have been shifted on the intensity axis for clarity.

Upon hydration of these same materials with D_2O as described above, at room temperature (23^oC) and at 60^oC , new d spacings were recorded at the block and cluster peaks emerged for some of the samples, showing the hierarchical structure. Figure 2 shows the SANS data obtained from FISS samples hydrated at these temperatures.

Since the contrast for these SANS experiments is from the D_2O absorbed into the hydrophilic domain, several trends may be observed as more of it is absorbed. It is expected that the contrast with the rest of the polystyrene in that domain should become sharper and the peak position may shift to lower q values. Also, since the D_2O is absorbed essentially in the hydrophilic domain, there will emerge a clear peak due to the block phase separation and a shift in the peak position as more D_2O is absorbed. This is observed clearly for the AC50 samples, where the block separation peak moved from a q value of 0.023710A^{-1} to 0.017699 A^{-1} when hydrated at 23^oC and at 60^oC respectively. This corresponds to d spacings of 26.5 nm and 35.5 nm respectively. Compared to the d spacing of 22.7 nm from the same sample in the dry state obtained by USAXS, these new d spacings represent an increase of 16.7% and 36.0% in center to canter distance of this sample. This indicates a clear trend of domain dilation with increased hydration.

A similar trend can be seen for the CS50 sample. In the dry state the block d spacing was 23.7nm from USAXS, whereas after soaking in D_2O at 23^oC, it increases to 27.8 nm representing a 17.3% increase. Upon soaking this sample at 60^oC it disintegrates and forms a swollen gel which shows a micelle-like scattering profile. Both the AC50 and CS50 curves loose their distinct hierarchical features when soaked at 60oc , confirming their change in structure. The AC28 and CS23 samples show essentially the same block phase separation peak position as they absorb relatively smaller amounts of D_2O (See Chapter 2).

On the cluster length scale the same trend can be seen. The CS50 sample which had a cluster d spacing of 3.2 nm in the dry state indicated by the broad peak at higher q[18], has a center shifted to approximately 5.8 nm upon soaking at 23°C. The AC50 sample which had not cluster peak in the dry state SANS, shows a 3.2nm spacing peak when soaked at 23°C, which becomes vague after soaking at 60°C. This is an indication of a coalescence process of the D_2O containing cluster pools, which blurs out individual cluster entities. This leads to a three dimensional network of hydrated channels, resulting in a jump of ionic conductivity. A similar structural evolution has been shown for Nafion[TM] upon increased hydration[13], which results in a percolation threshold in its ionic conductivity.

The change in domain spacing of AC28 and AC50 immersed in D_2O liquid and it's vapor at different relative humidity values are shown in Figure 3. The same trend of domain dilation, as indicated by first order peak maximum shift to low q, is seen as humidity is increased up till immersion in liquid. This domain dilation can is also more prominent for the higher sulfonated AC50 sample than for the AC28 sample as expected. The lower temperature and lower humidity (35% RH) spectra, show little or no change from the dry state.

The Half-width at half-maximum (HWHM) of the scattering peak gives a clear indication of the degree of order in a phase separated block copolymer system. Broader peaks indicate a more disordered liquid-like systems.[19,20]. As seen in Figure 2(a) the peak for AC50 samples are much broader than the CS50 samples, indicating a more disordered morphology, as seen also from TEM (See chapter 2). The broadness also indicated the presence of more deuterated water D_2O in this sample. Upon soaking in D_2O at 60°C the block domain peak further broadens out into a shoulder, confirming extensive loss of order and liquid-like structure. This can also be seen by the disappearance of a distinct cluster peak, supporting the suggestion that a three-dimensional network structure of hydrated channels has evolved. The domain dilation and coalescence of cluster pools to form conducting channels as described above, has been modeled in Figure 4 below. It must be borne in mind that the uptake of hydrophilic molecules in ionomers is closely related to temperature, and there is sometimes a precipitous change in swelling accompanying thermal transitions[21].

Thermal and Mechanical Transitions

The transition from a glassy to a rubbery state in an amorphous polymer or polymer segment can be detected through a change in heat capacity of the polymer, which is measurable by DSC. The DSC themograms of some of the dried as-received FISS materials are shown in Figure 5 for the second heating scan of a heat-cool-heat cycle. The AC28 and AC50 samples have similar glass transition (T_g) temperature at 45.3°C and 45.5°C, in good agreement with literature[22]. However the CS50 sample has a T_g of 32.6 °C for the FI block.. The difference between the cesium and the acid (proton) material transitions is likely due to the relatively more bulky cesium ions and the way it effects the whole chain mobility. The T_g of the sulfonated PS block was undetectable even when probed up to 170 °C, and may have been elevated beyond this temperature due to sulfonation as seen in other ionomers[23,24].

Upon a transition from the glassy state to the rubbery state in the fluorinated poly(Isoprene) block, which is the bulk phase of the polymer, the mechanical integrity of the whole PEM made from this material is compromised. This is shown in Figure 6 below in which the Storage modulus of the AC50 sample drops by more than 90% between 45°C and 60°C (at 1hz frequency). Since the storage modulus in viscoelastic solids measure the stored energy or the solid-like characteristic of a viscoelastic material[25], it means that this material will flow under desirable fuel cell membrane application temperatures (60°C-100°C), even without considering the softening effects swelling. On the other hand the Nafion^{TM}, though not as stiff at room temperature, maintains appreciable mechanical integrity under desirable use temperatures.

Membrane samples from the same batch used for the SANS experiments were soaked in the same manner in deionized water for 16 hours, at room temperature and at 60°C and the DSC thermograms obtained thereafter are shown in Figure 7. After soaking 20°C a depression in the glass transition of all the samples that were measured in the dry state was recorded. The data are summarized in Tables 3, and show that the highest T_g reduction of 6.2^{o}C was observed for AC50, which has the highest water uptake value for membranes soaked at 20°C. This indicated that the absorbed water serves as a plasticizer even in the hydrophobic FI domain. Similar glass transition reduction effects observed in other ionomer systems have been attributed to the presence of non-freezing water[27].

The state of water in the hydrophilic domains of an ionomer can be deduced from the characteristics of the melting endotherm, upon the melting of frozen absorbed water, via differential scanning calorimetry[26]. The occurrence of a broad melting endotherm between -20°C and 20°C, has been attributed to the melting of freezable water that is loosely bound to the polymer chains [28]. The same kind of features have been observed for the FISS samples soaked at 60°C and seen in Figure 7(b). The broadest peaks are observed for the samples with correspondingly large water uptake values, as can be seen in Table 3. The peak area gives a measure of the crystallization enthalpy (effectively how much water is bound to the acid sites of the ionomer), and shows that AC50 has the largest crystallization enthalpy and also the largest water uptake at this pre-soak temperature. No sharp spike can be seen in the thermograms suggesting the absence of free- water in the system. Nafion 112 membranes on the other hand show much less loosely bound water under the same conditions, than AC50. They were also much less visibly swollen after soaking at 60°C but had better transport properties, suggesting that they use the water they do absorb much more efficiently than the FISS-AC50 material. Also there is no glass transition observable in the FISS samples because they are, to varying degrees, essentially in the gel state upon soaking at 60°C.

Micelle Formation
Amphiphillic polymers and oligomers (surfactants) are well known to self assemble into various kinds of micelles in a liquid medium. In an aqeous medium, the hydrophilic part of the polymer would face the water, while shielding the hydrophobic portions of the chains in the micelle core, thus preventing unfavorable interactions with the water. Many types of micellar structures are known and well studied including

spherical, ellipsoidal, cylindrical, bilayer (vesicles), however for the most part they can be approximated as being spherical.

Small angle scattering is widely used as a tool for characterizing the size ,shape , and other features of these micellar aggregates. In our SANS experiments with FISS-CS97 materials, the contrast which leads to scattering is due to the difference in neutron SLD between D_2O and both the FI ans SS block of this highly sulfonated water soluble sample.. Calculations using SLD figures from Table 2,   show that the ratio SLD for D_2O versus FI block is 4.7, while for sPS (Cs^+) versus FI block is 1.3, therefore the strongest contrast is between the D_2O or aqueous surrounding medium and the FI chains in the core of the micelles. In this scenario the structure of the hydrophilic polymer chains in the micelle corona can also be determined as, they are an intermediate region between the core, and the D_2O only regions, this is known as shell contrast..

The SANS profiles for solutions of the CS97 samples with concentrations of 0.05, 1, and 10 mg/ml in D_2O are shown in Figure 8(a). The curves for 1, and 10 mg/ml solutions have essentially the same shape , with a form factor peak in the mid q range around the same position indicating they are have similar shapes and sizes. In the high q region, where the smallest features can be seen , the slopes of the curve indicate the conformation of the hydrophilic chains dangling in the D_2O. A I(q) dependence of q^{-2}, indicates gaissian chains whereas, a q^{-1} dependence indicates 1-dimensions objects, or stretched out chains[29]. The Power law fits to the data show, that the 1mg/ml solution have approximately q^{-1} dependence , whereas the 10mg/ml solution has q^{-2} dependence. This can be explained by the fact that the latter have less space for each micelle due to the higher concentration than the former, and so the chains have less room to stretch. The low concentration, 0.05 mg/ml solution has too little scattering to discern this slope due to very few scattering objects being present and hence low counting statistics.

The shape of micelles can be determined by the use of a kratky plot[30]. The kratky, I(q) x q^2 versus q plot for a spherical object exhibits a clear peak , with its position dependent on the objects radius of gyration. This is because the Gaussian coil (low q or guinier) portion of the curve is multiplied by relatively small q^2 value[31]. At higher angles, where the guinier approximation no longer holds , the curve should obey the porod approximation (I(q) α q^{-4}) and the intensity should sharply decease when multiplied by q^2, forming a peak. As can be seen for the Kratky plots in Figure 8(b), all the plots show a distinct peaks(the peak for the 0.05 mg/ml is visible at a smaller scale), confirming the micelles are essentially spherical. The peak for the 10mg/ml sample is positioned at slightly higher q value, indicating a smaller radius of gyration.

The size of a micelle can be determined from the net scattering intensity I(q) based on the Guinier approximation (at low q values) as expressed in the equation below:

$$I(q) \ = I(0) \exp (-R^2_g \ q^2/3) \tag{1}$$

Where I(0) denotes the scattering intensity extrapolated to zero angle and R_g is the radius of gyration. The initial slope in the logarithm plot of equation (1) gives the radius of gyration of the micelle[30]. The Guinier plots and analysis of the micelle data studied are

shown in Figure 8(c). The radius of gyration values for the 0.05, 1, and 10 mg/ml solution micelles are 13.3, 13.5 and 130 nm respectively. The results for the 0.05 and 1 mg/ml solutions are almost the same, with the largest size of 13.5nm for the 1mg/ml sample. The size for the 10mg/ml sample is slightly smaller, further confirming the suggestion that the 1mg/ml has stretched out chains which may increase its radius of gyration, whereas the 10mg/ml samples may experience some crowding effects and so show a smaller radius of gyration with Gaussian, random coils.

Conclusions

SANS and USAXS have been used to study the structural evolution of FISS materials as they have evolved from the dry state to the water soluble state. A dilation of the nanometer-scale hydrophilic domains has been observed as hydration was increased, with higher swelling for the higher sulfonated samples or upon hydrating at higher temperatures. Furthermore a decrease in the order in these microphase separated structures is reduced upon dilation. The glass transition temperature of the fluorinated blocks, have been seen to decrease upon hydration of these materials; and at the highest hydration levels DSC has shown the presence of tightly bound water. A precipitous drop in the mechanical integrity of the AC50 materials is also observed upon exceeding its T_g.. These results explain the bursting of the membranes during methanol permeability testing at 60^oC, and the sharp increase in methanol permeability with increased temperature. To further develop these materials, new approaches must be found to limit the domain dilation, and increase the glass transitions way beyond the operating temperature.

Finally highly sulfonated CS97 samples have shown self-assembly into spherical micelles in aqueous media, even at concentrations as low as 0.05 mg/ml. This is related to the highly dissimilar blocks (fluoropolymer versus ionic) in these ionomer. The sizes of these micelles range from 13-13.5 nm, with the higher concentration solutions having smaller radius of gyration, possibly due to crowding effects.

References
(1)   http://www.freepatentsonline.com/6140436.html
(2)   Longworth, R.; Vaughan, D.J. Polym. Prepr. (Am. Chem. Soc. , Div. Polym. Chem.) **1968**, 9, 525.
(3)   Eisenberg, A. *Macromolecules* **1970**, 3, 147.
(4)   Semonov, A. N.; Nyrkova, I.A.; Kholkhov, A. R. Macromolecules **1995**, 28, 7491.
(5)   Gierke, T.D.; Munn, G.E.; Wilson, F.C. *J. Polymer Sci: Polym. Phys. Ed.* **1981**, 19, 1687.

(6)   Hickner, M. A.; Ghassemi, H.; Kim, Y. S.; Einsla, B.R.; McGrath, J. E. *Chemical Reviews* ,**2004**, 104,.4587.
(7)   O'Hayre, R. P.; Cha, S.; Cololla, W.; Prinz, F.B. In *Fuel Cell Fundamentals* ; 1 ed.; John Wiley& Sons, Inc: New York ,**2006**; p 15.
(8)   Yang, Y.; Holdcroft, S. *Fuel Cells* **2005**, 5,171.

(9)   Lu, X.; Steckle, W.P. Weiss, R.A. *Macromolecules* **1993** 26, 5876.
(10)   Williams, C.E.; Russell, T.P.; Jerome, R.; Horrion, J. *Macromolecules* **1986,** 18, 2877.
(11)   Bishop, M.T.; Karasz, F.E.; Russo, P.S.; Langley, K.H. *Macromolecules*. **1985** ,18, 86.
(12)   Tricoli, V. *J. Electrochem. Soc.* **1998,** 145, 3798.
(13)   Gebel, G. *Polymer* **2000**, 41, 5829.
(14)   Huang ,T.; Gido, S.P.; Mays, J.W. *Synthesis and Characterization of Fluorinated and Sulfonated Block Copolymers for Fuel Cell Proton Exchange Membrane*, Unpublished manuscript.
(15)   Miyake, N.; Wainright, J.S.; Savinell, R.F. *J. Eletrochem. Soc.* **2001**, 148, A898.
(16)   The OMEGA® Temperature Handbook and Encyclopedia, Vol. MMV™ 5th Edition[®]
(17)   http://www.isis.rl.ac.uk/largescale/loq/documents/sans.htm
(18)   Peiffer, D.G.; Weiss, R.A.; Lundberg, R.D. J. Polym. Sci., Polym. Phys. **1982**, 20, 1563.
(19)   Ryu, D.Y.; Jeong, U.; Kim, J.K.; Russell, T.P. Nature Materials **2002**,1, 114.
(20)   Rodriguez-Abreu, C.; Lazzari, M.; Varade, D. ; Kaneko, M ; Aramaki, K. ; Quintela, M.A.L. Colloid Polym. Sci. **2007**, 285, 673.
(21)   Kreuer, K.D. Solid State Ionics **1997**, 97, 1.
(22)   Ren, Y.; Lodge, T.P; Hillmyer, M.A. J. Am. Chem. Soc. **1998**,120, 6830.
(23)   Weiss, R.A.; Sen, A.; Pottick, L.A.; Willis, C.L. Polymer 1991, 32, 2785.
(24)   Rigdahl, M.; Eisenberg, A. J. Polym. Sci., Polym. Phys. Edn. **1981**, 19,1641.
(25)   Meyers, M.A.; Chawla, K.K. Mechanical Behaviour of Materials, Prentice Hall, 1999, 98. Hickner et al. Fuel Cells **2005**, 5, 213.
(26)   Kim, Y.S.; Dong, L.; Hickner, M.A.; Glass, T.E.; Webb, V.; McGrath, J. E. Macromolecules **2003**, 36 6281.
(27)   Nakamura, K.; Hatakeyama, T.; Hatakeyama, H. Polymer **1983**,24, 871.
(28)   Kataoka,M.; Hagihara, Y.; Mihara, K.; Goto, Y J. Mol. Biol. **1993**, 229, 591.
(29)   Sugiura, S. et al. J. Coll. Interf. Sci. 2001, 240, 566.
(30)   Flanagan, J.M.; Kataoka, M.; Fujisawa, T. Engelman, D.M. Biochemistry 1993, 32, 10359.

Table 1   Dry sample center-to-center distances for fluorinated poly(Isoprene)-*block*-sulfonated poly(Styrene) (FISS) obtained by USAXS.

Sample	D spacing of Block, nm	D spacing of Cluster, nm
FISS-AC28	20.3	4.7
FISS-CS23	20.3	4.7
FISS-AC50	22.7	
FISS-CS50	23.7	3.2

Table 2   Neutron Scattering length densities calculated for different parts of fluorinated poly(Isoprene)-*block*-sulfonated poly(Styrene) and D_2O.

Scattering Unit	D_2O	FI	PS	sPS (H^+)	sPS (Cs^+)
Neutron SLD* (cm^{-2} x 10^{-11})	0.6236	0.1313	0.1374	0.2519	0.1764

* Calculated using scattering cross section data from T. P Russell's, Polymer Physical Chemistry lecture notes and Reference 16.
FI: fluorinated poly(Isoprene)
PS: poly(Styrene)
sPS (H^+): sulfonated poly(Styrene) with proton counterion
sPS (H^+): sulfonated poly(Styrene) with cesium counterion

Table 3   Thermal properties of fluorinated poly(Isoprene)-*block*-sulfonated poly(Styrene) and Nafion^{TM}.

Polymer	Dry Thickness (υm)	Water Uptake (%)		Glass Transition Dried(°C)	Glass Transition after soaking (°C)	Tg Reduction after soaking (°C)	Area/Water absorbed after soaking (J/g)
		20°C[b]	60°C[b]	105°C[c]	20°C[b]	20°C[b]	60°C[b]
Nafion 112	50						0.11
FISS-AC50	81	17	595	45.5	39.3	6.2	74.45
FISS-CS50	91	5	a	32.6	32.4	0.2	a
FISS-AC28	69	5.4	257	45.3	41.9	3.4	54.86
FISS-CS23	74	2.4	129				7.34

[a]Not Measurable

[b]Pre-soak Temperature in Deionized water

[c]Pre-Dry Temperature under N_2 flow
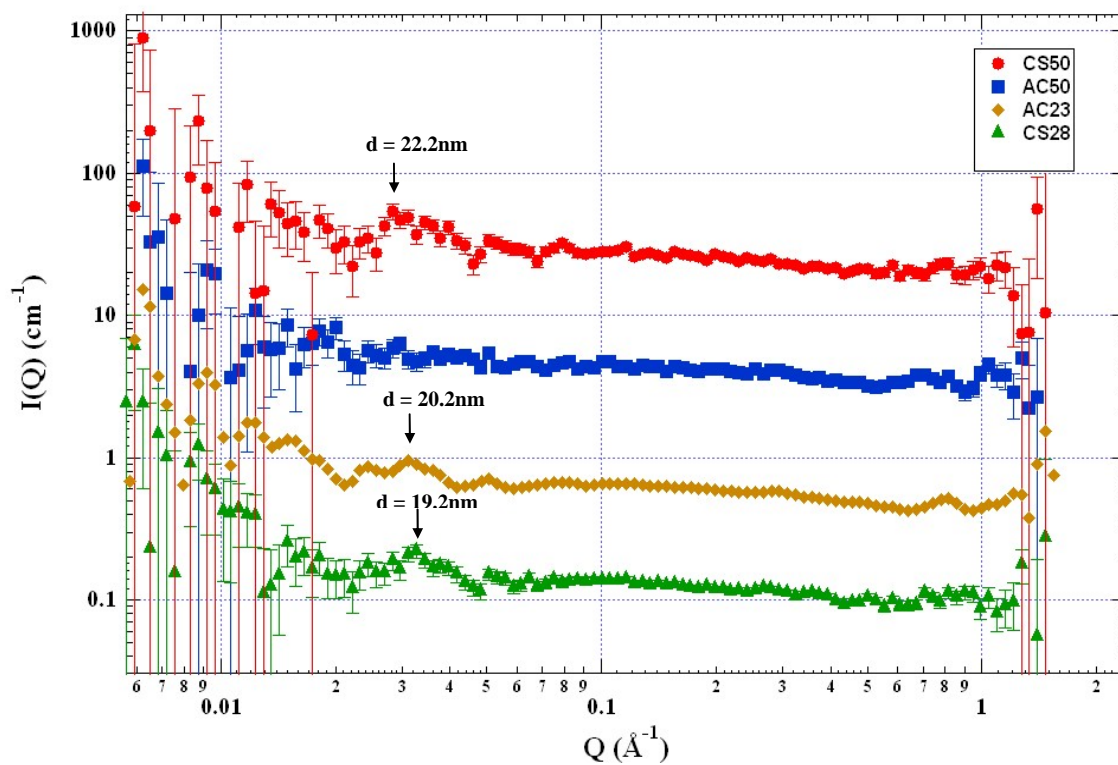
Figure 1 SANS profiles from fluorinated poly(Isoprene)-*block*-sulfonated poly(Styrene) dry at 23°C.
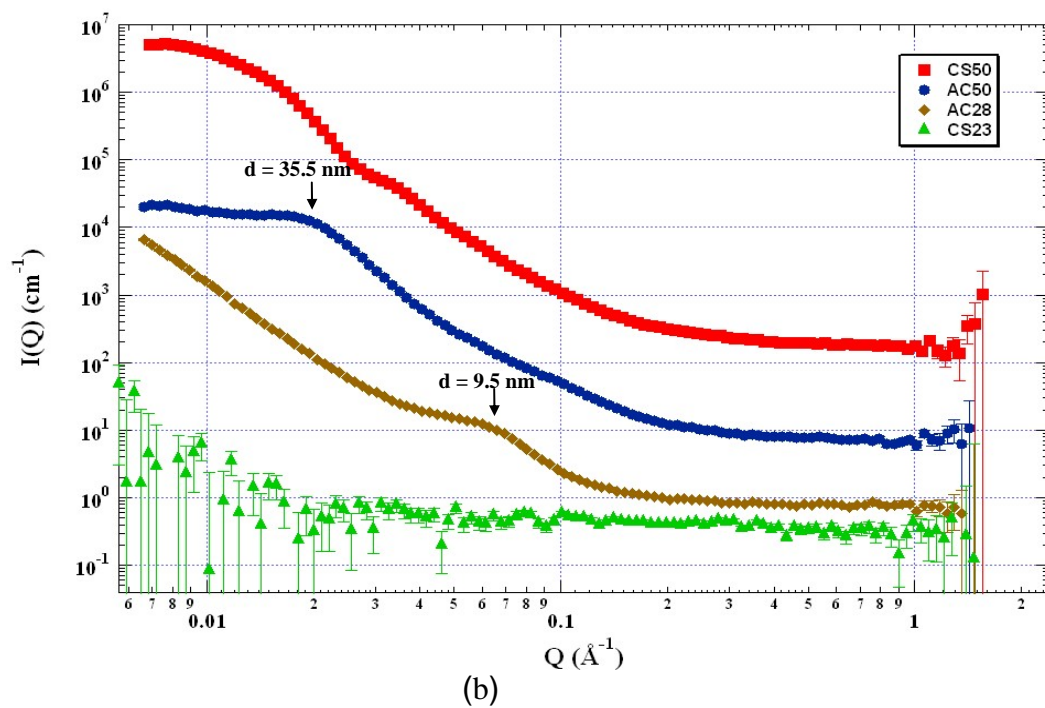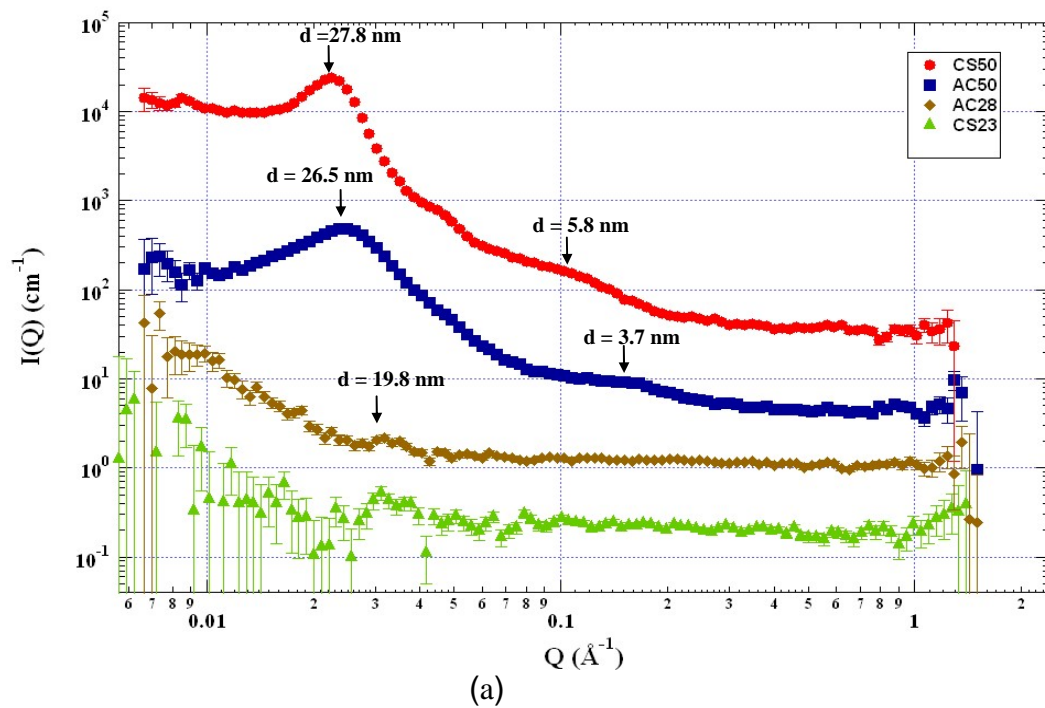
Figure 2 SANS profiles from fluorinated poly(Isoprene)-*block*-sulfonated poly(Styrene) soaked for 16 hours in D_2O at (a) 23^oC and (b) 60^oC.
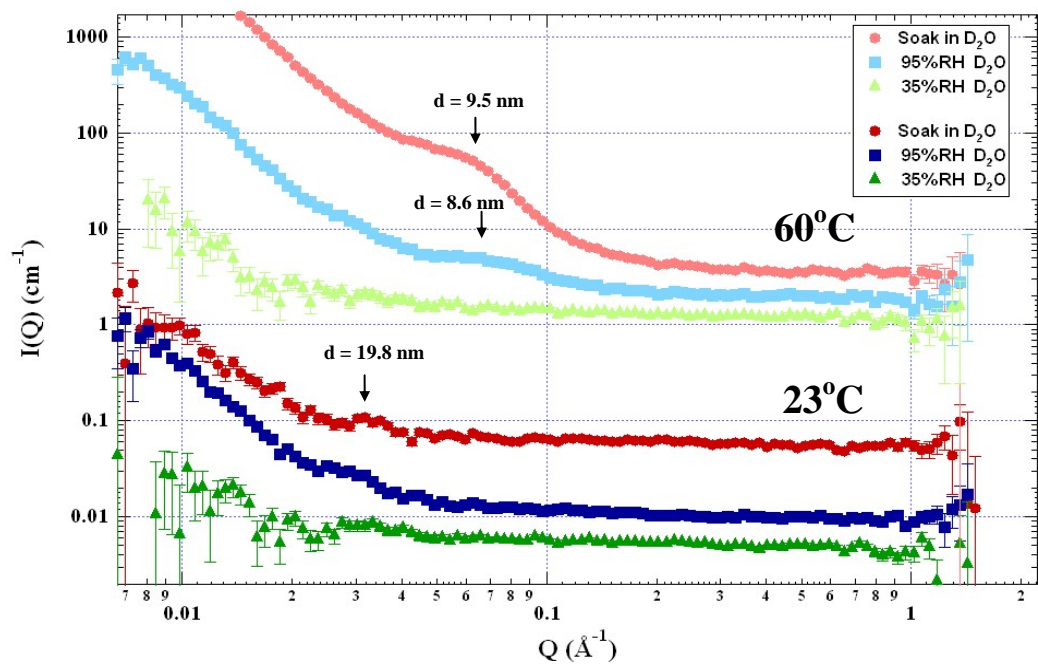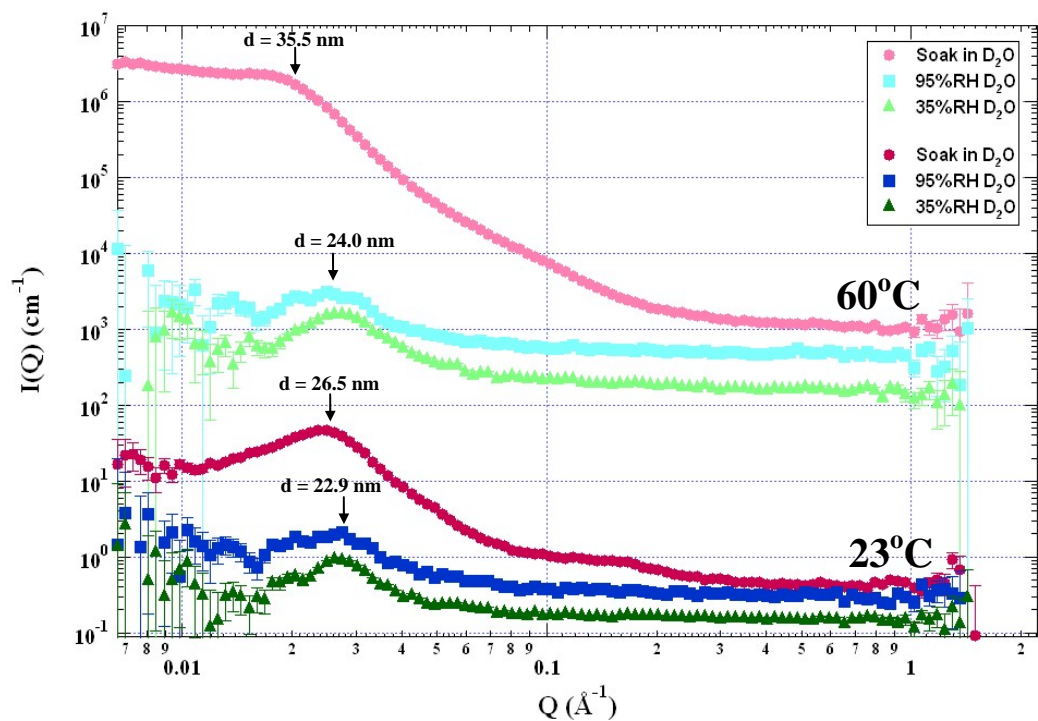
Figure 3 SANS profiles from fluorinated poly(Isoprene)-*block*-sulfonated poly(Styrene) soaked for 16 hours in D_2O and its vapor for (a) AC28 and (b) AC50.
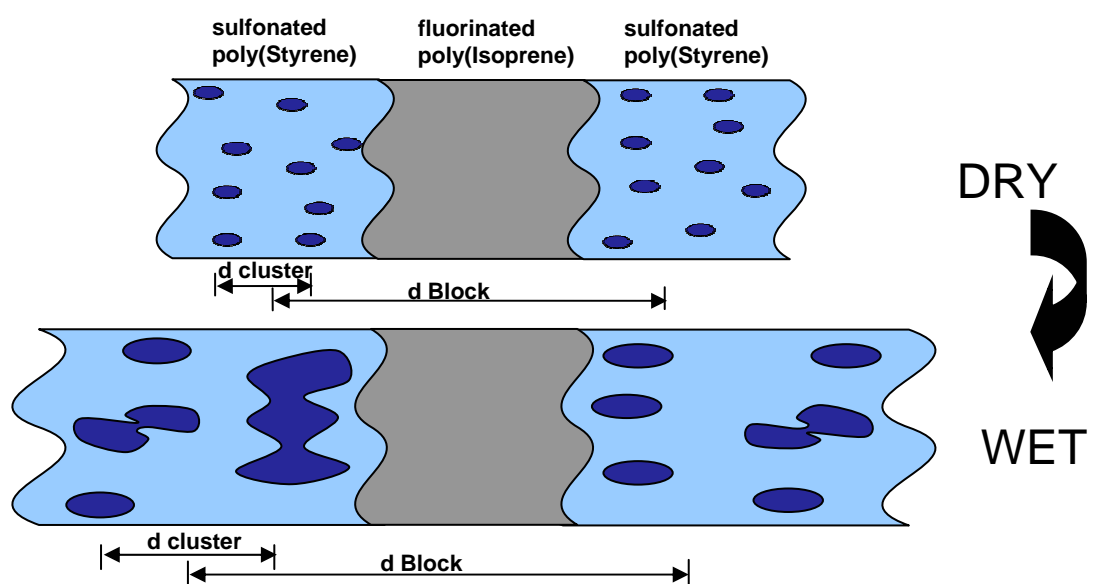
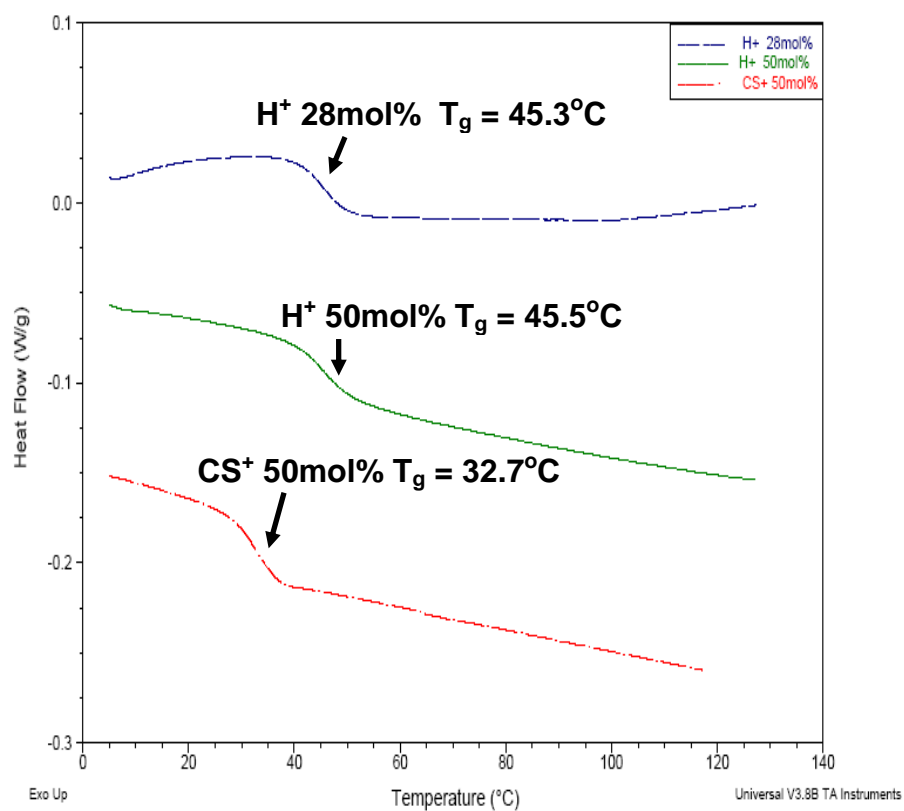Figure 4 Schematic of structural evolution with increased hydration.

Figure 5 DSC thermogram from fluorinated poly(Isoprene)-*block*-sulfonated poly(Styrene) as received samples dried under nitrogen flow overnight at 105°C.
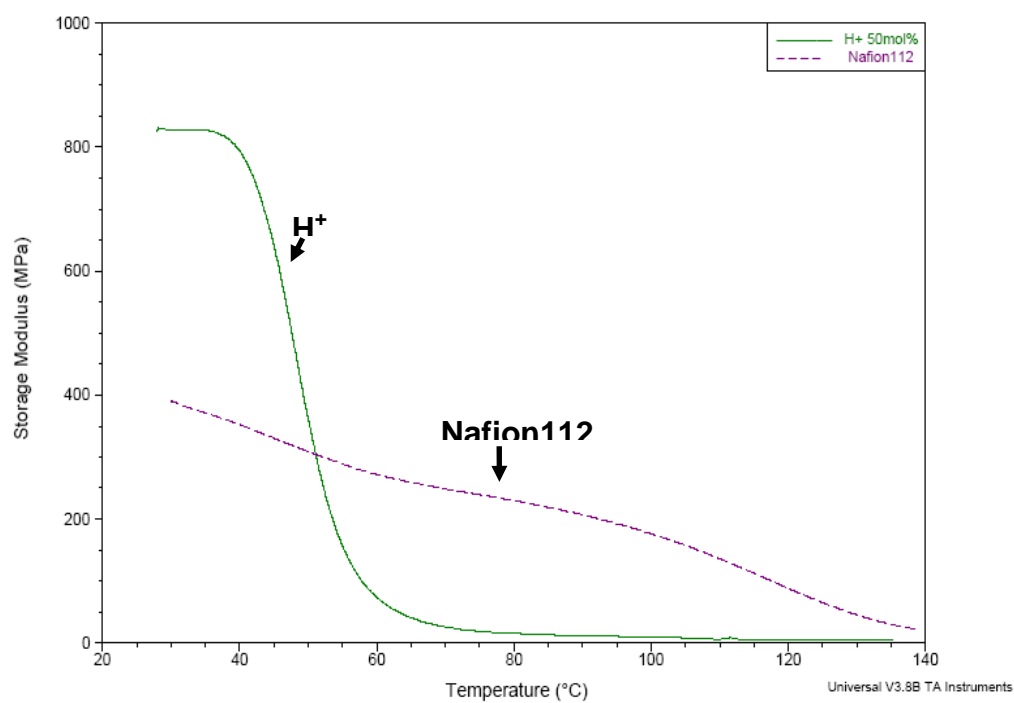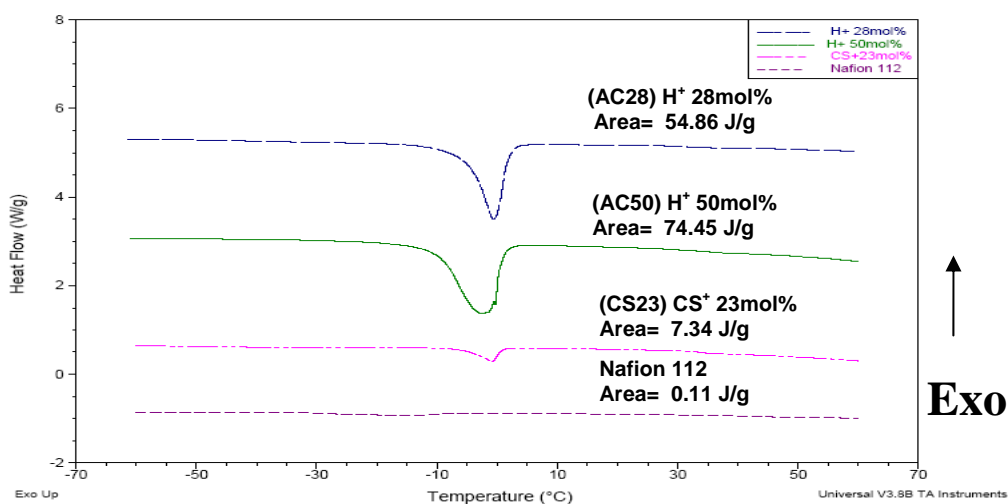
Figure 6 DMTA curves for fluorinated poly(Isoprene)-*block*-sulfonated poly(Styrene) and Nafion[TM] samples pre-dried under nitrogen flow overnight at 105°C. Tension Mode.
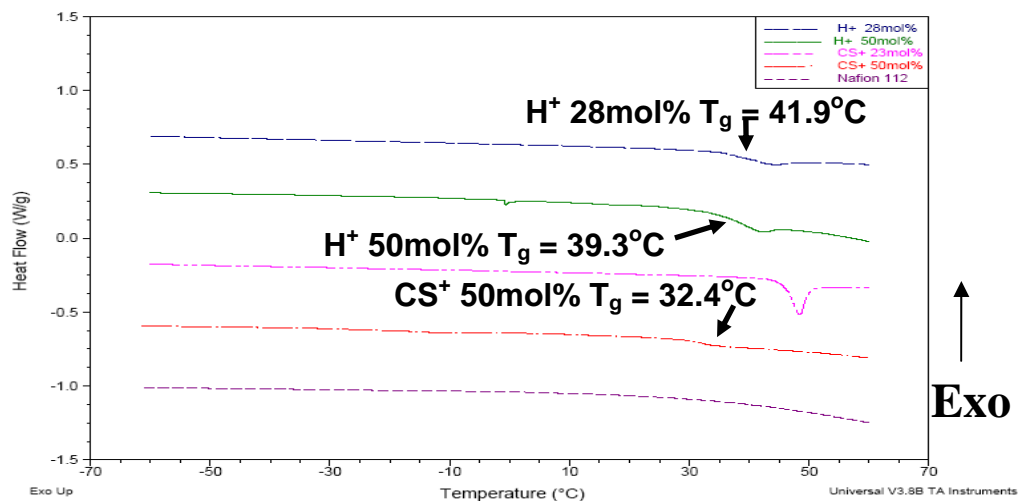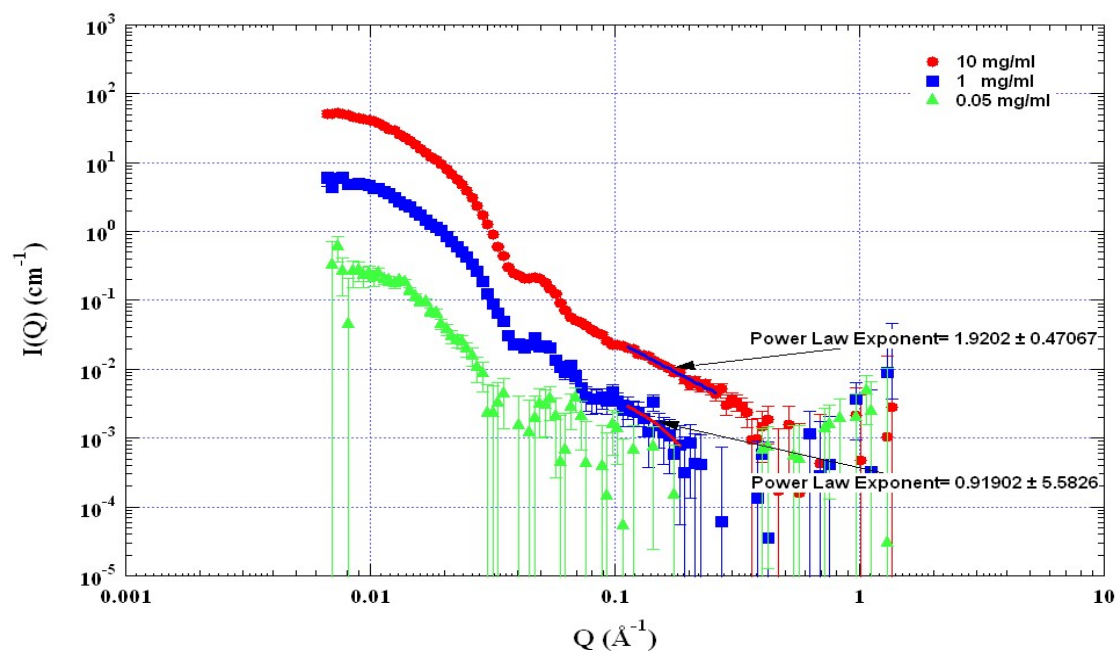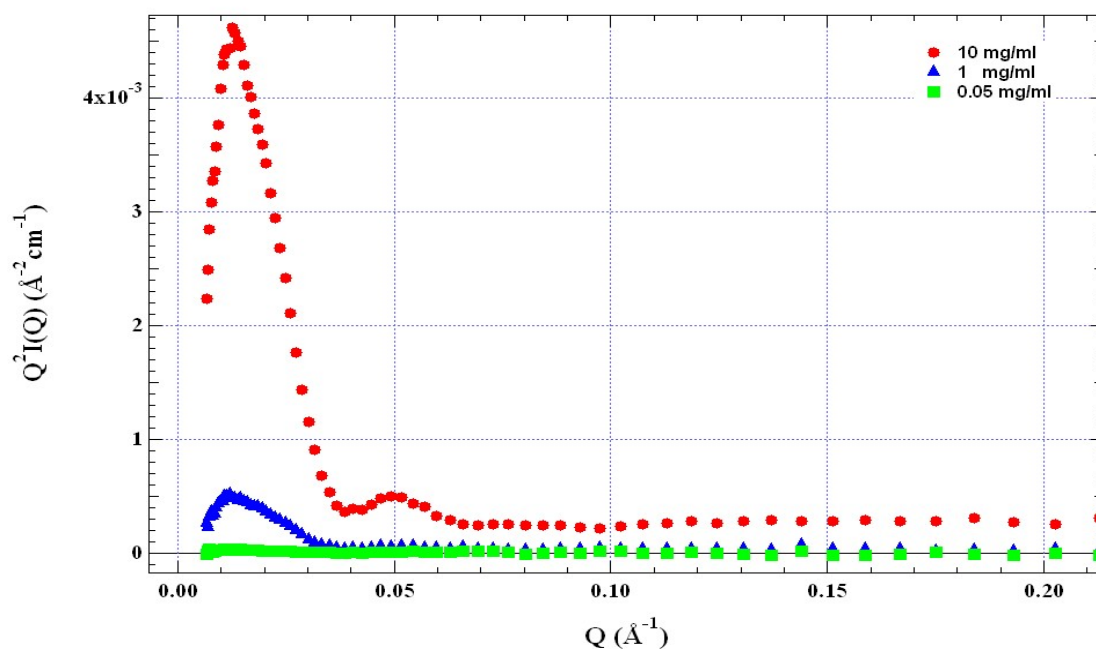
(a)

(b)

Figure 7 DSC thermograms from fluorinated poly(Isoprene)-*block*-sulfonated poly(Styrene) soaked for 16 hours in H_2O at (a) 23^oC and (b) 60^oC.
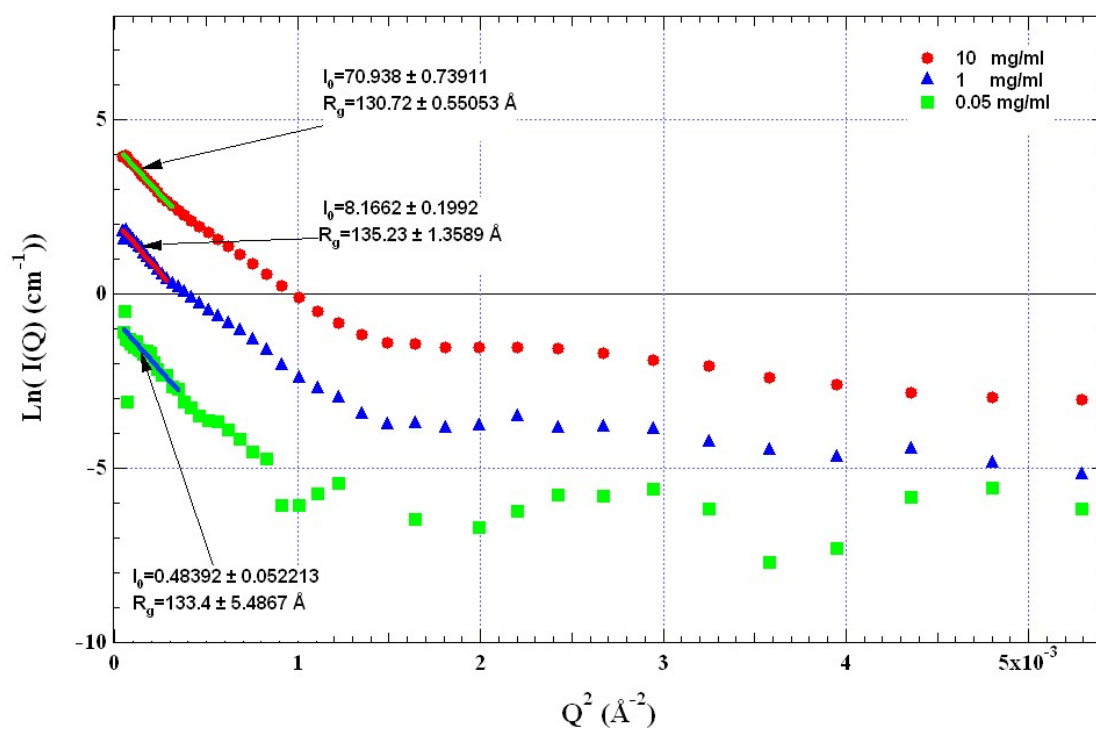
(a)

(b)

Figure 8 SANS profiles from fluorinated poly(Isoprene)-*block*-sulfonated poly(Styrene) micelles formed in D$_2$O (a) profiles with Power law fits (b) Kratky plots (c)Guinier plots and analysis. (Continued)

$I_0=70.938 \pm 0.73911$
$R_g=130.72 \pm 0.55053$ Å

$I_0=8.1662 \pm 0.1992$
$R_g=135.23 \pm 1.3589$ Å

$I_0=0.48392 \pm 0.052213$
$R_g=133.4 \pm 5.4867$ Å

10   mg/ml
1   mg/ml
0.05 mg/ml

Q^2 (Å^{-2})

Ln(I(Q) (cm^{-1}))

(c)

Figure 8 (Continued)

(5.3) POLYMER ELECTROLYTE MEMBRANES FROM FLUORINATED POLY(ISOPRENE)-BLOCK-SULFONATED POLY(STYRENE): MICRODOMAIN ORIENTATION BY EXTERNAL FIELD.

Abstract

In this study, block copolymer ionomers of the cesium salt (20 mol %) of fluorinated poly(Isoprene)-block-sulfonated poly(Styrene) have been spun cast into membranes and annealed under an electric field of ~40 V/um at 130oC for 24hours. This resulted in the .transformation of the morphology from a random phase separated state to one preferentially oriented in the direction of the electric field but with smaller domain sizes. The effect of this change in morphology was a 2.5 times increase in the ionic conductivity as measured by electrochemical impedance spectroscopy, at all humidity conditions measured. This can be attributed to the increased connectivity of the ionic domains. This technique may find application in the fabrication of nanostructured polyelectrolytes with enhanced charge transport capacity.

Introduction

The use of external fields to orient the different components of a polymeric system has gained significant interest over the last decade. It involves the application of an external field to induce structural rearrangement of a material to achieve preferential texture in a desire direction. Different kinds of external field have been employed including shear[1,2], electric fields[3-5], solvent evaporation[6,7], and mechanical constraints[8,9].and magnetic fields[10].These techniques commonly employ the interaction of the field with the anisotropic portions of the materials having different components that are not phase mixed such as blends, block copolymers, or polymer- nanoparticle mixtures.

The purpose of such microdomain orientation is typically to enhance orientation dependent properties, and has found application in the fabrication of templating nanowire arrays[11,12], photonic crystals[13,14], and improved gaseous permeability[15]. The effective diffusion of small molecules through polymeric microdomains has been shown to vary inversely to the square of tortuosity[16], where tortuousity is a measure of the degree of twisting of the domains. In essence a block copolymer with oriented domains has been shown to have much higher transport of the penetrant small molecules in the direction of orientation.

This same approach has been applied to the improvement of ionic conductivity. A study by Weiss and Coworkers et al.[17,18] showed that blend of sulfonated Poly (Ether Ketone Ketone) ionomer and neutral Poly (Ether Imide) cast under an electric field(E-field), yielded a morphology with the ionic component oriented in the direction of this E-field (Perpendicular to plane of membrane) and resulted in orders of magnitude increase

in ionic conductivity. Also LiI:PEO based solid Polymer electrolyte for batteries showed one- order of magnitude increase in Li ion conductivity upon orientation of the PEO crystalline chains, by incorporation of magnetic particles and application of a magnetic field[19]. Furthermore it has been predicted that an orientation of block copolymer ionomer domains in the direction of desired ionic conductivity would enhance their utility as Polymer electrolyte fuel Cell membranes[20].

Block copolymers are particularly suited for microdomain orientation by external fields, due to their predictable formation of microstructures with anisotropic domains, such as lamellae or hexagonally packed cylinders. Much work has been done on the orientation of block copolymers using E-Fields. Most of the work has centered on poly(Styrene)-poly(Methyl Methacrylate) (PS-b-PMMA) block copolymers[3,5,21,22], and their complexes with Lithium salts[23]. Some work has also been done on rubbery di- and tri-block copolymers of poly(Styrene)-poly(Isoprene), as well as poly(Styrene)-poly(Ethylene-co-butylene)- poly(Styrene) (sSEBS) as shown in Figure 1.

The driving force for the alignment of block microdomains is due to the dielectric constant difference between the dissimilar blocks. Recent experimental studies in the melt have suggested that disordering of the original lamellar morphology is followed by rotation of the smaller grains formed in the direction of the applied E-field[24,25], whereas studies from solution suggest the latter step is preceded by defect translation[26]. These suggested pathways have also been corroborated by simulation[27,28].

Few studies have been reported on the orientation of ionomers by any external field[29,30]. This was found to be a nontrivial task as the ionic aggregation of the acid sites severely limited chain mobility, in nematic liquid crystal domains. Alternatively track-etched membranes with pores oriented normal to the plane of the membrane , have been filled with ionomers, yielding significant increase in ionic conductivity compared to isotropic membranes[31,32]. This work is focused on the orientation of block copolymer ionomer domains normal to the plane of membranes formed from them and investigation of the resultant effects on proton conductivity.

Experimental Section
Materials
The synthetic procedure and characterization for fluorinated poly(Isoprene)-block- sulfonated poly(styrene) (FISS) materials have been described in detail elsewhere[33]. The precursor poly(styrene)-block- poly(Isoprene) (PS-PI) diblock copolymer used in this work was anionically polymerized, having reported characteristics: Mw =27,000 ,PDI=1.05, 50mol% PS. The fluorinated samples had the PS block sulfonated to 20 mol%, as determined by ^{1}H NMR, and subsequently neutralized to the cesium salt form. This sample will be referred to as FISS-CS20 hereafter.

Preparation of Membrane
Membranes from the FISS-CS20 samples were prepared by spin coating a 5 wt % solution in Tetrahydrofuran (THF) unto a silicon substrate on which gold had been deposited, as shown in Figure 2 below. Spin speed was at 1000 rpm and was left to spin

for 5mins. The resultant film was ~ 500nm in thickness as determined by a Dektak[3] profilometer. A piece of this membrane coated wafer was reserved as the As-cast sample.

E-field Alignment Experiments

An aluminized Kapton film was used as an upper electrode , having ~ 25 υm layer of crosslinked poly(Dimethylsiloxane) (PDMS) (Slygard) cured on the kapton side. This was necessary to have an intimate contact between the top electrode and the copolymer film , thus eliminating insulating air gaps. The sandwitched capacitor, was placed in an oven with a nitrogen flow blanket, and annealed at 130°C for 24 hours under an E-field strength of ~ 40V/υm as shown in Figure 3. The E-field was typically applied before the oven got heated. The whole setup was quenched to room temperature before the applied E-field was removed.

Transmission Electron Microscopy (TEM).

TEM samples were prepared from both the As-Cast and E-Field samples. A thin layer of gold, and then carbon was sputtered unto the surface of the membrane still in the gold coated wafer. The gold serves as a membrane edge marker, while the carbon serves as an epoxy diffusion barrier. Both samples were then embedded and cured in room temperature cure Epoxy for 24 hours. The membrane was then separated from the substrate by immersing in liquid nitrogen, and subsequently 50 nm thin sections of the sample were cut across the thickness of the membrane (E-field direction) using a Leica Ultracut UCT cryomicrotome at -120°C. These were then collected on copper grids and stained with RuO_4 vapor for 1 hour. It is assumed that only the unsulfonated polystyrene domains were stained. TEM images were obtained using a JEOL-2010 microscope operating at an accelerating voltage of 200KV in the bright field mode.

Ionic Conductivity

Ionic (cesium) conductivity of the membranes were measured by means of two probe complex impedance spectroscopy techniques, which measure conductivity normal to the plane of the membrane respectively. Pieces of both the As-cast and E-field samples still on the gold plated substrates were immersed in a chamber with 50% relative humidity (RH) for 24 hours, and then rapidly sandwiched between another piece of gold coated silicon wafer (gold face touching membrane). A solartron 1252A frequency response analyzer linked to a an SI 1287 electrochemical interface was used within a frequency range of 0.1 and 300KHz, and the value of the real intercept in the imaginary vs. real impedance plot (Bode plot) in the high frequency range is taken as the bulk resistance of the membrane to ionic conductivity, as described in elsewhere[34]. The same test was repeated for the same samples after soaking in a 100% RH chamber for 7 hours.

Results and Discussion

The value of orientation of ion conducting domains in the direction of the desired ion transport has been demonstrated for batteries and for fuel cell polymer electrolytes. However facile direct methods to orient block copolymer ionomers, which have increasing appeal as fuel cell membrane materials due to their fast and predictable self-assembly into nanometer lengthscale structures, are still lacking. The above described

experiments were carried out to investigate the viability of electric field induced alignment in this regard.

Cross sectional TEM micrographs of FISS-CS20 samples, which were spun coated, and subsequently annealed under an electric field are shown in Figure 4 below. The as-cast samples show a randomly (mixed) oriented morphology, with the dark portion being the sulfonated Poly(styrene) domains. This is the typical cylindrical morphology expected from a elastomer-styrene block copolymer with a PS minor component of around 25-27mol % as shown in Figure 1(a). The rapid spin coating and solvent evaporation results in a kinetically trapped morphology.

Upon annealing of an uncharged block copolymer under an electric field, an orientation of the domains in the direction of the electric field is achieved, by one of the mechanisms discussed earlier, as seen in Figure 1(b). It is observed that the orientation of the domains does not visibly affect the domain size. However, upon application of a similar treatment to the sulfonated FISS-CS20 samples, there is a visible reduction in the domain size as seen in Figure 4(b). This results in a much finer grained morphology, and essentially a greater degree of connectivity in the hydrophilic domains.

Also it has been shown that the order in self assembled morphologies observed in cast block copolymers ionomers is reduced upon annealing[35]. This observed change is related to the fact that the electrostatic interactions leading to the formation of ionic clusters are much stronger than the weak non-covalent interactions that lead to block copolymer phase separation. These behave as physical cross links, hence reducing the mobility of the chains and hindering their self assembly into equilibrium structures[36]. So upon annealing the polymer chains gain energy for increased mobility, and this allows the ionic groups to come in the vicinity of one another more often and interact, locking in a structure at a shorter length scale (see chapter 3) than for block phase separation, in a random fashion. This then templates the self-assembly of the block copolymer dissimilar chains which are chemically connected together, in an equally random fashion, at a lenghtscale limited by the molecular dimensions. This process may play a significant part in the smaller, grainy morphology observed upon annealing of the FISS-CS20 samples.

On the other hand, a slight preferential orientation of these grainy domains can be observed in the direction of the applied E-field (indicated by the arrow). This orientation is by no means complete or exclusive, as it is the result of competition between electrostatically induced random orientation; and polarization of the anisotropic microphase structure by the electric field inducing alignment in its direction. The dominant effect will depend on field strength, temperature of annealing, duration of annealing, and ionic content to varying degrees. A more extensive and systematic study will be required to decouple and quantify the influence of each.

The ionic (cesium) conductivity of As-Cast and E-field annealed FISS-CS20 samples from different pieces of the same spin-coated silicon substrate, has been measured across the plane of the membrane, and results are shown in Figure 5. The data clearly indicates an increase in conductivity of ~ 2.5 times upon annealing under an

electric field over the as-cast samples. The low absolute figures are either due to the low relative mobility of the heavy cesium ion being measured, or the low humidity or hydration condition, however the increase in conductivity is consistent for both humidity conditions measured.

This increase in conductivity may be attributed to the high domain connectivity, in the grainy random morphology of the Efield annealed sample or due to the induced preferential orientation in the electric field direction, which is also the direction in which ionic conductivity was measured. An increase in conductivity can however be the result of either of these morphological attributed or both. A more exhaustive study of this approach to increasing conductivity in block ionomers will be required, however this approach shows significant promise as a facile means of creating nanostructured ionomer membranes with controlled orientation.

Conclusions

Annealing of cesium salt (20 mol %) of fluorinated Poly(Isoprene)-block-sulfonated poly(Styrene) transforms its morphology from a random phase separated state to one preferentially oriented in the direction of the electric field but with smaller domain sizes. This morphological change can be tentatively attributed to a competition between templating intermolecular electrostatic interactions of the ionic groups on the sulfonated blocks and the polarization of the dissimilar block domains in the electric field. The effect of this change in morphology is a 2.5 time increase in the ionic conductivity as measured by electrochemical impedance spectroscopy, at all the humidity conditions measured. This can be attributed to the increased connectivity of the ionic domains.

References
(1)   Schmidt,G.; Richtering, W.; Lindner, P.; Alexandridis, P. Macromolecules **1998**, 31, 2293.
(2)   Zipfel, J.; Berghausen, J.; Schmidt, G.; Lindner, P.; Alexandridis, P. Tsianou, M.; Richtering, W. Phys. Chem.. Chem. Phys. **1999**, 1, 3905.
(3)   Amundson, K. et al. Macromolecules **1991** , 24, 6546.
(4)   Amundson, K. ; Helfand, E. ; Quan, X. ; Smith , S.D.; Macromolecules **1993**, 26 2698.
(5)   Morkved, T.L.; Lu, M.; Urbas, A.M.; Ehrichs, E.E.; Jaeger, H.M.; Mansky, P.; Russell, T.P. Science **1996**, 273, 931.
(6)   Kim, G.; Libera, M. Macromolecules 1998, 31, 2569.
(7)   Kim, S.H.; Misner, M.J.; Xu, T.; Kimura, M.; Russell, T.P.; Adv. Mater. **2004** 16, 226.
(8)   Kofinas, P.; Cohen, R.E. Macromolecules 1994 , 24, 3002.
(9)   Zhao, Y.; Roche, P.; Yuan, G. Macromolecules **1996**, 29, 4619.
(10)   Grigorova, T.; Pispas, S.; Hadjicristidis, N., Thurn-Albrecht, T. Macromolecules, 2005, 38, 7430.

(11)   Thurn-Albbrecht, T. et al. Science **2000**, 290, 2126.
(12)   Lopes, W.A. ; Jaeger, H.M. Nature **2001**, 414, 735.
(13)   Van Blaaderen, A.; Wiltzius, P. Adv. Mater. **1997**, 9 833.
(14)   Zhong, Y.; Wu, L.; Su, H.; Wong, K.S.; Wang, H. Optics Express **2006**, 14, 6837.
(15)   Drzal, P.L.; Halasa, A.F.; Kofinas, P. Polymer **2000**, 41, 4671.
(16)   Faridi, N.; Duda, J.L.; Hadj-Romdhane, I. Ind. Eng. Chem. Res. **1995**, 34, 3556.
(17)   Weiss, R.A. et al. DOE Hydrogen Program FY **2004** Progress Report.
(18)   Bellows, R. et al. DOE Hydrogen Program FY **2004** Progress Report.
(19)   Golodnitsky, D.; Livshits, E.; Kovarsky, R.; Peled, E.; Chung, S.H.; Suarez, S.; Greenbaum, S.G. Electrochem. and Solid State Letters **2004**, 7, A412.
(20)   Elabd, Y.A.; Walker, C. W.; Beyer, F. L. J. Membr. Sci. **2004**, 231, 181.
(21)   Thurn-Albbrecht, T. ; DeRouchey, J. Russell,T.P. ; Jaeger, H.M. Macromolecules **2000**, 33, 3250.
(22)   Xu, T. et al. Macromolecules **2005**, 38, 10788.
(23)   Wang, J. ; Leiston-Belanger, J.M. ; Sievert, J.D. ; Russell, T.P Macromolecules **2006**, 39, 8487.
(24)   Xu, T. ; Zhu, Y. ; Gido, S.P. ; Russell, T.P. Macromolecules **2004**, 37, 2625.
(25)   DeRouchey, J. ; Thurn-Albrecht, T. ; Russell, T.P.; Kolb, R. Macromolecules 2004 37 2538.
(26)   Boker, A.; Knoll, A.; Elbs, H.; Abetz, V.; Muller, A.H.E.; Krausch, G. Macromolecules 2002, 35, 1319.
(27)   Tsori, Y.; Andelman, D. Macromolecules **2002**, 35, 5161.
(28)   Zvelindovsky, A.V.; Sevink, G.J.A. Phys. Rev. Lett. **2003**, 90, 049601.
(29)   Yuan, G.; Zhao, Y. Polymer **1995**, 36, 2725.
(30)   Roche, P.; Zhao, Y. Macromolecules **1995**, 28, 2819.
(31)   Chen, H.; Palmese, G.R.; Elabd, Y.A. Chem. Mater. **2006**, 18, 4875.
(32)   Fang, Y.; Leddy, J. J. Phys. Chem.. **1995**, 99, 6064.
(33)   Huang ,T.; Gido, S.P.; Mays, J.W. *Synthesis and Characterization of Fluorinated and Sulfonated Block Copolymers for Fuel Cell Proton Exchange Membrane*, Unpublished manuscript.
(34)   See Chapter 2: Experimental Section.
(35)   Mani, S.; Weiss, R.A.; Williams, C.E.; Hahn, S.F. Macromolecules 1999 32, 3663.
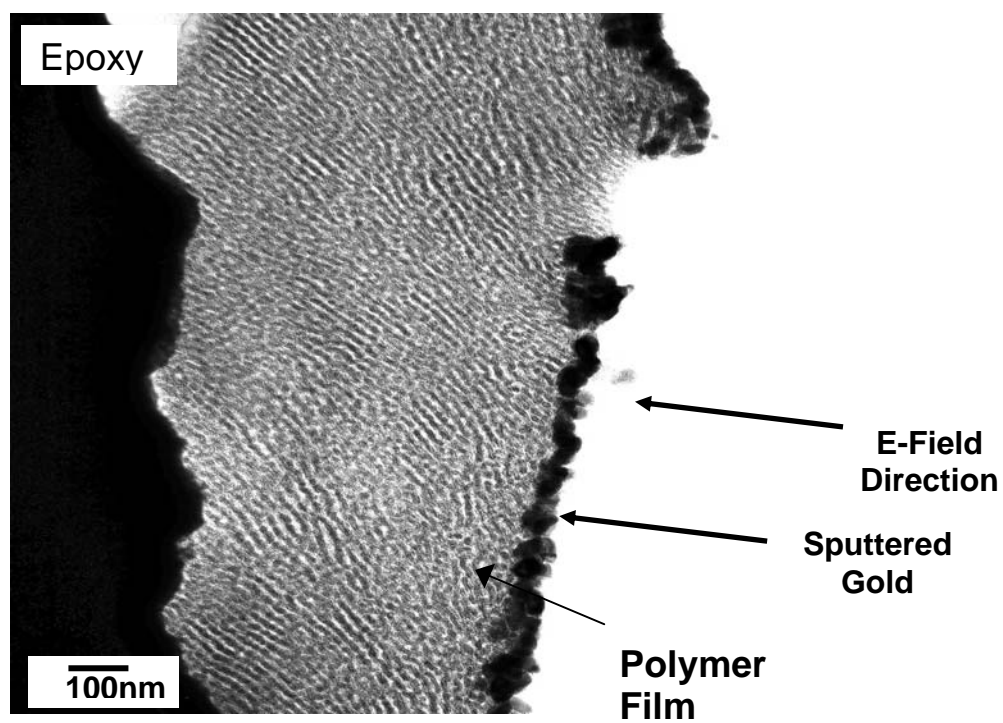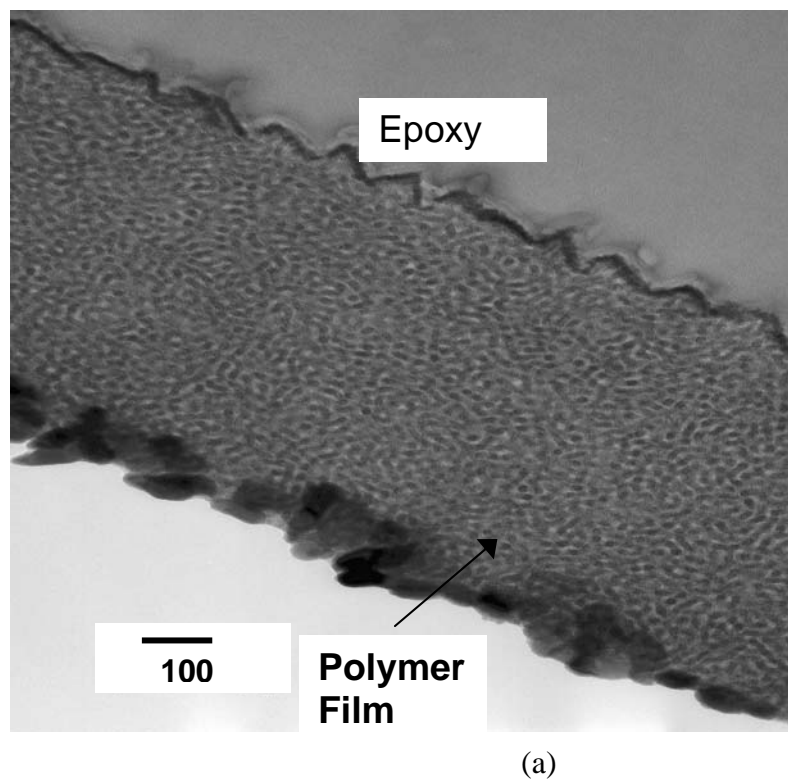(36)   Blackwell, R.I.; Mauritz, K.A. Polymer 2004, 45, 3457.

(a)

(b)

Figure 1 TEM micrographs showing sSEBS samples (a) As-Cast , (b) After Electric field of ~ 45V/um applied at 208°C, for 24 hours.
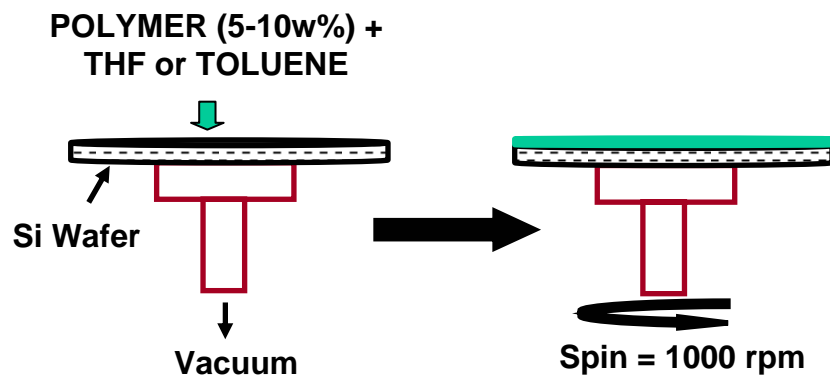
**POLYMER (5-10w%) +
THF or TOLUENE**

Si Wafer

Vacuum

Spin = 1000 rpm

Figure 2 Schematic of spin casting operation.

Electric Field Apparatus

N₂

Oven

Aluminum

Kapton Film 25.4 um

PDMS

Polymer Sample

SiO2   2nm

Si Wafer

DC
Power Source/
Transformer
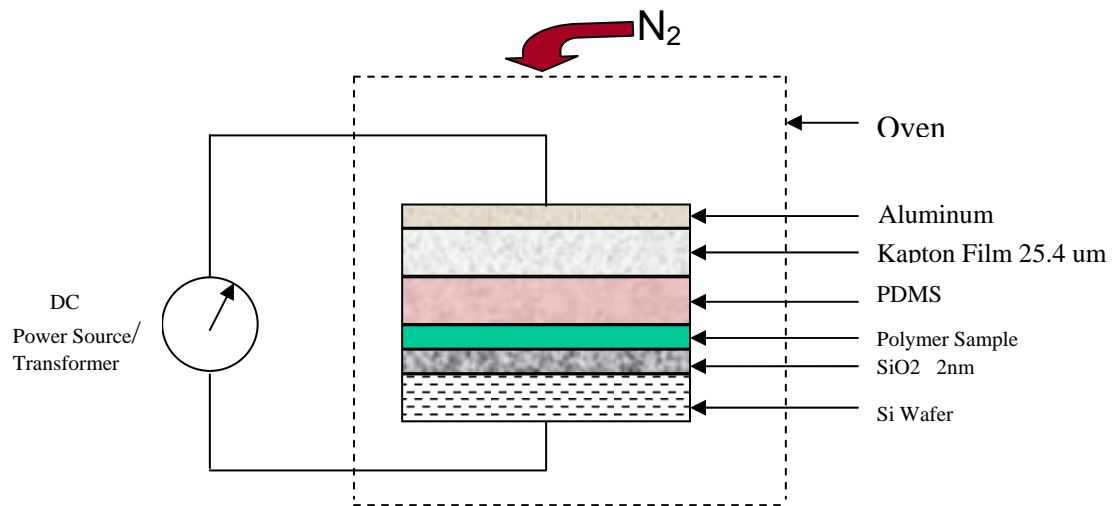
Figure 3 Schematic of Electric Field Alignment Experimental Setup.

Epoxy

Sputtered
Gold

Polymer
Film

50 nm
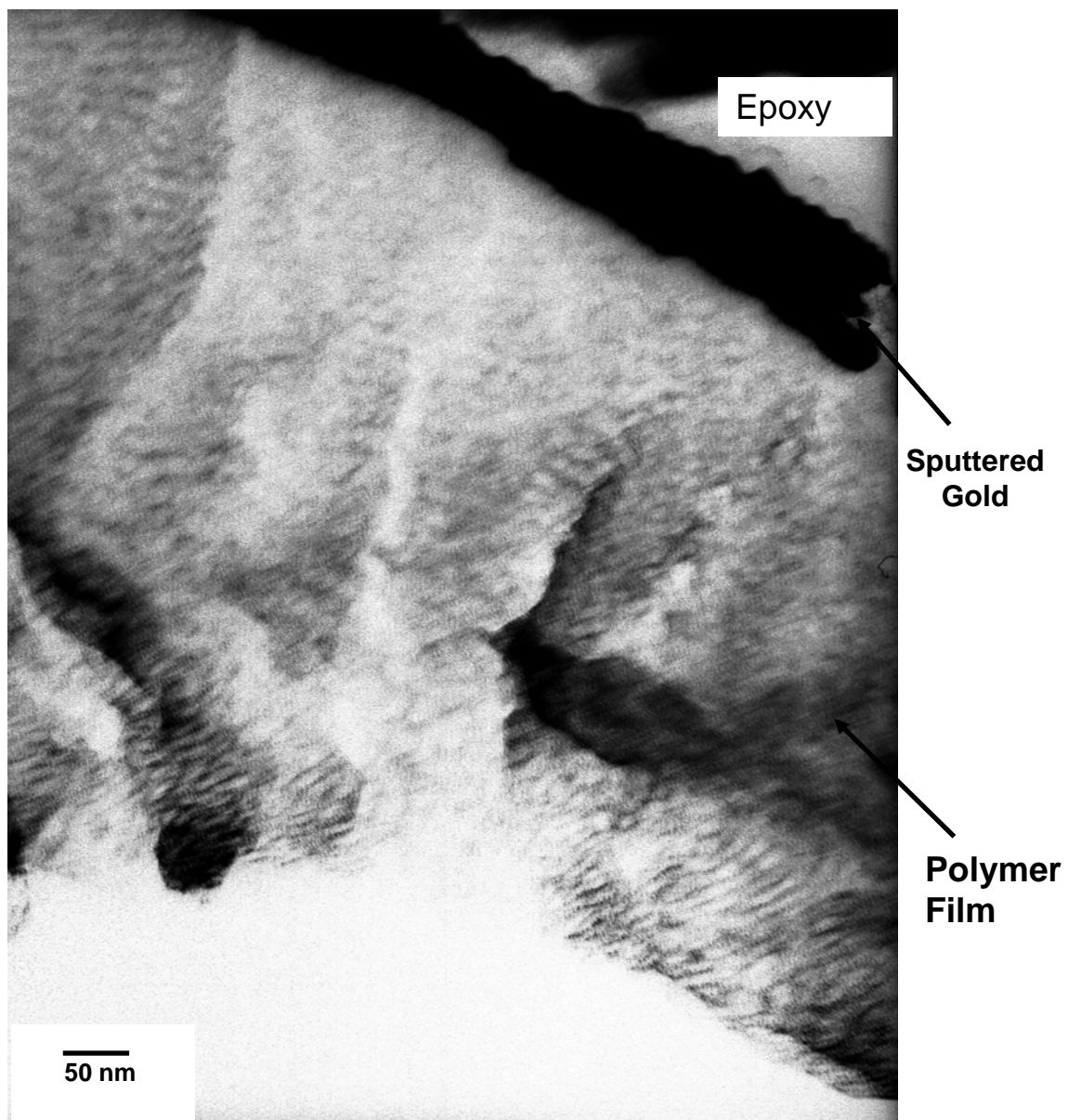
(a)

Figure 4 TEM micrographs showing FISS-CS20 samples (a) As-Cast , (b) After annealing under Electric field of ~ 40V/um applied at 130oC, for 24 hours. (Continued).

E-Field Direction

Polymer Film

50 nm
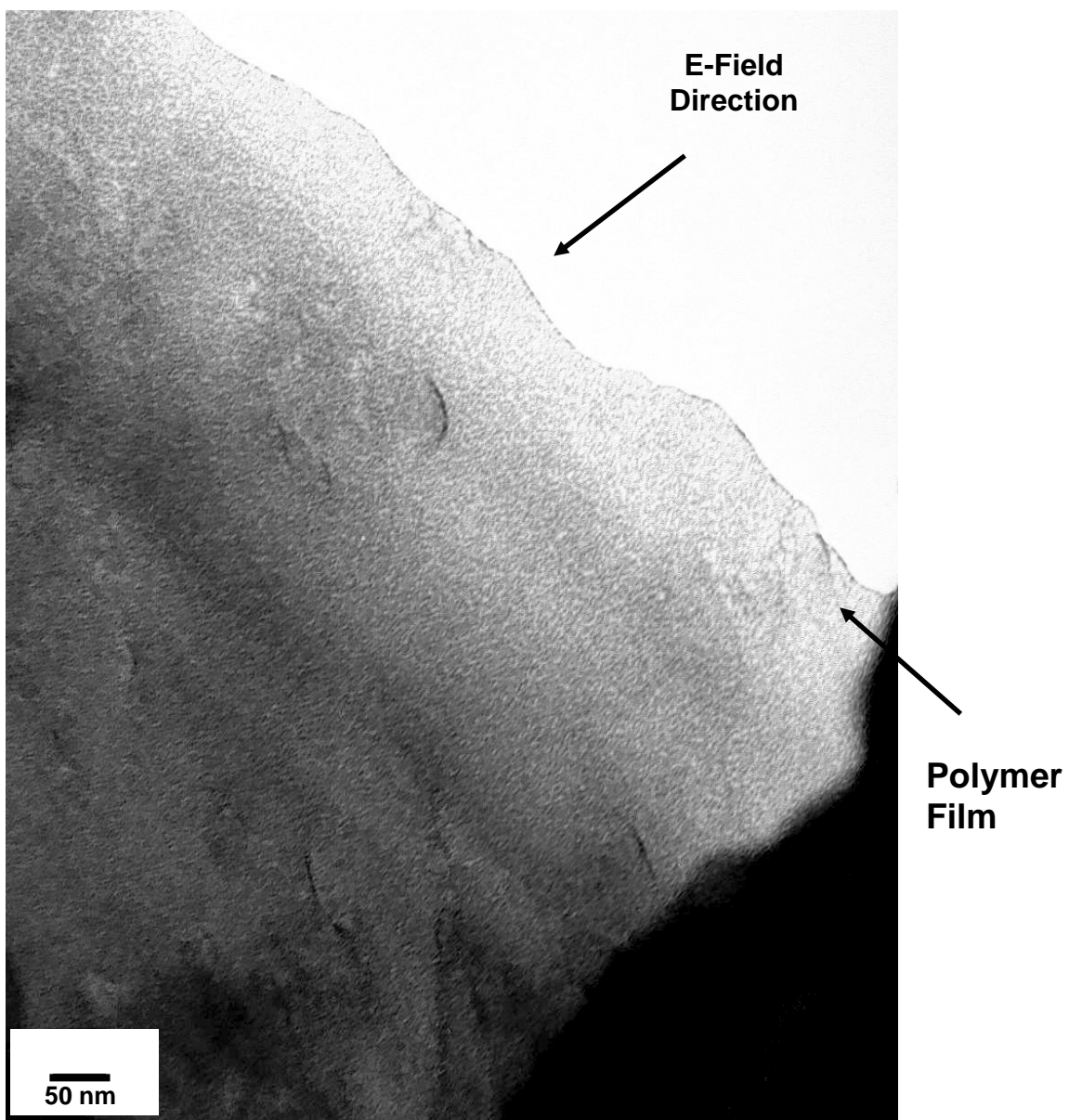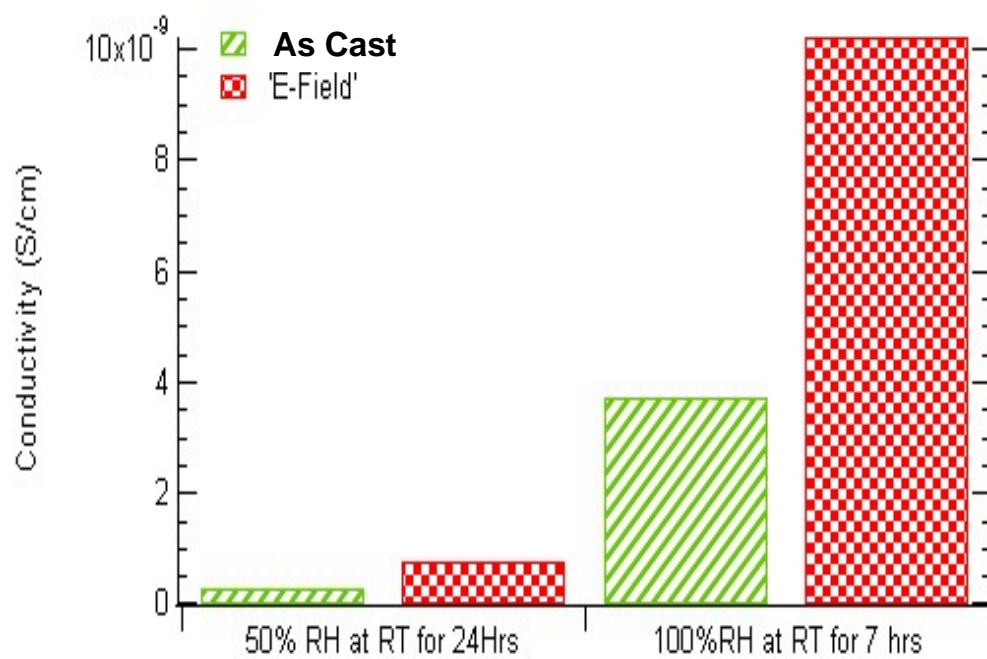
(b)

Figure 4 Continued.

Figure 5 Ionic (cesium) conductivity results for As-Cast and Efield annealed FISS-CS20 samples.